Article

Compositional and Electric Field Dependence of the Dissociation of Charge Transfer Excitons in Alternating Polyfluorene Copolymer/Fullerene Blends

Dirk Veldman, O#zlem I#pek, Stefan C. J. Meskers, Jo#rgen Sweelssen, Marc M. Koetse, Sjoerd C. Veenstra, Jan M. Kroon, Svetlana S. van Bavel, Joachim Loos, and Rene# A. J. Janssen

J. Am. Chem. Soc., **2008**, 130 (24), 7721-7735 • DOI: 10.1021/ja8012598 • Publication Date (Web): 22 May 2008

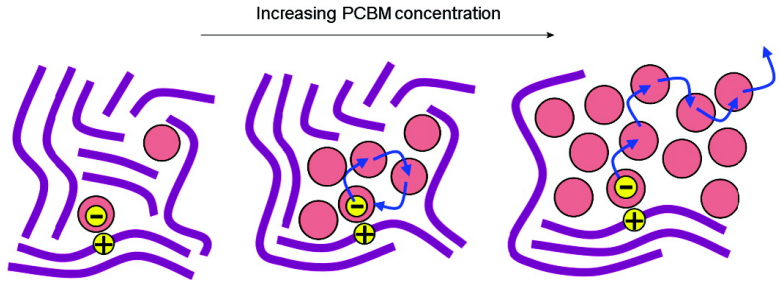

More About This Article

Additional resources and features associated with this article are available within the HTML version:

- Supporting Information
- Links to the 3 articles that cite this article, as of the time of this article download
- Access to high resolution figures
- Links to articles and content related to this article
- Copyright permission to reproduce figures and/or text from this article

View the Full Text HTML

J|A|C|S
ARTICLES

Published on Web 05/22/2008

Compositional and Electric Field Dependence of the Dissociation of Charge Transfer Excitons in Alternating Polyfluorene Copolymer/Fullerene Blends

Dirk Veldman,[†] Özlem İpek,[†] Stefan C. J. Meskers,[†] Jörgen Sweelssen,[‡,||] Marc M. Koetse,[‡,||] Sjoerd C. Veenstra,[§,||] Jan M. Kroon,[§,||] Svetlana S. van Bavel,[#,||] Joachim Loos,[#,||] and René A. J. Janssen*[,†]

Molecular Materials and Nanosystems, Eindhoven University of Technology, P.O. Box 513, 5600 MB Eindhoven, The Netherlands, Holst Centre/TNO, High Tech Campus 48, 5656 AE Eindhoven, The Netherlands, Energy Research Centre of The Netherlands (ECN), P.O. Box 1, 1755 ZG Petten, The Netherlands, Dutch Polymer Institute, 5600 AX Eindhoven, The Netherlands, and Materials and Interface Chemistry, Eindhoven University of Technology, P.O. Box 513, 5600 MB Eindhoven, NL-5600 MB, The Netherlands

Received February 20, 2008; E-mail: r.a.j.janssen@tue.nl

Abstract: The electro-optical properties of thin films of electron donor−acceptor blends of a fluorene copolymer (PF10TBT) and a fullerene derivative (PCBM) were studied. Transmission electron microscopy shows that in these films nanocrystalline PCBM clusters are formed at high PCBM content. For all concentrations, a charge transfer (CT) transition is observed with absorption spectroscopy, photoluminescence, and electroluminescence. The CT emission is used as a probe to investigate the dissociation of CT excited states at the donor−acceptor interface in photovoltaic devices, as a function of an applied external electric field and PCBM concentration. We find that the maximum of the CT emission shifts to lower energy and decreases in intensity with higher PCBM content. We explain the red shift of the emission and the lowering of the open-circuit voltage (V_{OC}) of photovoltaic devices prepared from these blends with the higher relative permittivity of PCBM ($\varepsilon_r = 4.0$) compared to that of the polymer ($\varepsilon_r = 3.4$), stabilizing the energy (E_{CT}) of CT states and of the free charge carriers in blends with higher PCBM concentration. We show that the CT state has a short decay time ($\tau =$ ca. 4 ns) that is reduced by the application of an external electric field or with increasing PCBM content. The field-induced quenching can be explained quantitatively with the Onsager−Braun model for the dissociation of the CT states when including a high electron mobility in nanocrystalline PCBM clusters. Furthermore, photoinduced absorption spectroscopy shows that increasing the PCBM concentration reduces the yield of neutral triplet excitons forming via electron−hole recombination, and increases the lifetime of radical cations. The presence of nanocrystalline domains with high local carrier mobility of at least one of the two components in an organic heterojunction may explain efficient dissociation of CT states into free charge carriers.

I. Introduction

The most efficient polymer solar cells to date use a phase-separated composite blend of two materials with complementary electron donating and electron accepting properties. Excitons created by absorption of light in either of the two materials give rise to charge formation when they diffuse to the interface of the two components and are dissociated by a charge transfer reaction. The photogenerated holes and electrons are then transported and collected at opposite electrodes to sustain a photovoltaic effect. In general, polymer solar cells use a conjugated, semiconducting *p*-type polymer as electron donor, while the electron acceptor is either a small molecule (e.g., a fullerene derivative), a second conjugated *n*-type polymer, or an inorganic nanocrystalline semiconductor (e.g., CdSe or ZnO).[1]

Among the various materials combinations that have been investigated, blends of conjugated polymers with the electron accepting C_{60}-fullerene derivative [6,6]-phenyl-C_{61}-butyric acid methyl ester (PCBM), or its C_{70} analogue, take a prominent place because they provide power conversion efficiencies (η) that presently exceed 5%.[2] Within this class, the most exten-

[†] Molecular Materials and Nanosystems, Eindhoven University of Technology.
[‡] Holst Centre/TNO.
[||] Dutch Polymer Institute.
[§] Energy Research Centre of The Netherlands.
[#] Materials and Interface Chemistry, Eindhoven University of Technology.

(1) (a) Coakley, K. M.; McGehee, M. D. *Chem. Mater.* **2004**, *16*, 4533–4542. (b) Günes, S.; Neugebauer, H.; Sariciftci, N. S. *Chem. Rev.* **2007**, *107*, 1324–1338.
(2) (a) Peet, J.; Kim, J. Y.; Coates, N. E.; Ma, W. L.; Moses, D.; Heeger, A. J.; Bazan, G. C. *Nat. Mater.* **2007**, *6*, 497–500. (b) Laird, D.; Vaidya, S.; Li, S.; Mathai, M.; Woodworth, B.; Sheina, E.; Williams, S.; Hammond, T. *Proc. SPIE-Int. Soc. Opt. Eng.* **2007**, 6656–6659. (c) Wang, E.; Wang, L.; Lan, L.; Luo, C.; Zhuang, W.; Peng, J.; Cao, Y. *Appl. Phys. Lett.* **2008**, *92*, 033307. (d) Green, M. A.; Emery, K.; Hishikawa, Y.; Warta, W. *Prog. Photovolt: Res. Appl.* **2008**, *16*, 61–67.

10.1021/ja8012598 CCC: $40.75

sively studied materials combinations are blends of PCBM with poly[2-methoxy-5-(3,7-dimethyloxtyloxy)-1,4-phenylene vinylene] (MDMO-PPV) or regioregular poly[3-hexylthiophene] (P3HT) that provide $\eta = 2.5-3\%$,[3] and $\eta = 4-5\%$,[4] respectively. In these devices, charge generation and collection is very efficient as evidenced by internal quantum efficiencies that approach unity for the best devices. Despite these high quantum efficiencies, the process of charge separation from the interface in these devices and its dependence on the composition are only partially understood.

For MDMO-PPV:PCBM blends photoexcitation is followed by ultrafast ($\tau = 45$ fs) photoinduced charge transfer producing MDMO-PPV radical cations and PCBM radical anions with high efficiency, effectively quenching any competing photophysical pathway.[5] As the photoinduced electron transfer occurs over short distances, the initially created state will be characterized by a short electron−hole distance. At such short distance (e.g., 1 nm) the electron and hole are expected to be Coulombically bound by an energy (~0.5 eV) that exceeds thermal energy (~0.025 eV). This poses an intriguing question: how can electrons and holes effectively dissociate from the interface and how is geminate recombination of initially created electron−hole pairs prevented.

This crucial question has been addressed by several authors.[6] Mihailetchi et al. have developed a model, based on Onsager−Braun theory,[7] describing the dissociation of Coulombically bound electrons and holes by an external electric field to explain the current density−voltage ($J-V$) curves of organic photovoltaic devices.[8] Using electron and hole mobilities determined by space charge limited current (SCLC) measurements on actual photovoltaic devices, they fit the experimental $J-V$ characteristics using the rate for geminate charge recombination (k_F) as a parameter. For MDMO-PPV:PCBM excellent agreement was found for $\tau_F = k_F^{-1} = 2.5-40$ μs.[9] More recently this model has also been used to describe P3HT:PCBM[10] and polymer:polymer[11] blends. In the latter case a very long decay time ($\tau_F = 10$ ms)[11] is required to describe the $J-V$ characteristics. Other device models also often use charge carrier lifetimes on the order of microseconds.[12]

These long decay times strongly contrast with results from transient spectroscopy on conjugated oligo(*p*-phenylene vinylene)-fullerene and oligothiophene-fullerene dyads that show recombination of the charge separated state within 100 ps.[13] In addition, transient absorption studies on electron donor−acceptor blends reveal that charge recombination, either geminate or nongeminate, already occurs in the nanosecond time domain.[14,15] Time-delayed collection field measurements offer a separate method to determine the lifetime of charge carriers and show that at a delay time of 1 μs after photoexcitation of MDMO-PPV:PCBM blends, less than 0.5% of the charge carriers survive.[16] Although long-lived (up to the microseconds) charge carriers have frequently been observed in these electron donor−acceptor blends, there is little evidence that they represent a significant fraction (e.g., 10% or more) of the initially created photoinduced charge carriers.

Apart from these apparent discrepancies, another captivating issue in the field of polymer:PCBM photovoltaic blends is the relatively high fullerene content required to achieve high performance. For the semicrystalline P3HT:PCBM blends[4] the optimal ratio is approximately 1:1, but for many other, often amorphous polymers, the optimal ratio is around 1:4 by weight.[1] In each case the optimal PCBM concentration is much higher than the percolation threshold (17 vol % for spheres). Since PCBM gives only a small contribution to the total absorption of light and has a high electron mobility compared to the hole mobility of most polymers, a PCBM concentration higher than ~50 wt % would not be expected to increase the performance. For MDMO-PPV:PCBM blends a relation was found between the morphology of the active layer and device performance.[17,18] Only at high loading (>50 wt % PCBM) phase separation occurs, and essentially pure nanocrystalline PCBM domains form in an intimately mixed MDMO-PPV:PCBM blend. The

(3) (a) Shaheen, S. E.; Brabec, C. J.; Sariciftci, N. S.; Padinger, F.; Fromherz, T.; Hummelen, J. C. *Appl. Phys. Lett.* **2001**, *78*, 841–843. (b) Wienk, M. M.; Kroon, J. M.; Verhees, W. J. H.; Knol, J.; Hummelen, J. C.; van Hal, P. A.; Janssen, R. A. J. *Angew. Chem., Int. Ed.* **2003**, *42*, 3371–3375. (c) Mozer, A.; Denk, P.; Scharber, M.; Neugebauer, H.; Sariciftci, N. S.; Wagner, P.; Lutsen, L.; Vanderzande, D. *J. Phys. Chem. B* **2004**, *108*, 5235–5242.

(4) (a) Schilinsky, P.; Waldauf, C.; Brabec, C. J. *Appl. Phys. Lett.* **2002**, *81*, 3885–3887. (b) Padinger, F.; Rittberger, R. S.; Sariciftci, N. S. *Adv. Funct. Mater.* **2003**, *13*, 85–88. (c) Ma, W.; Yang, C. Y.; Gong, X.; Lee, K.; Heeger, A. J. *Adv. Funct. Mater.* **2005**, *15*, 1617–1622. (d) Li, G.; Shrotriya, V.; Huang, J.; Yao, Y.; Moriarty, T.; Emery, K.; Yang, Y. *Nat. Mater.* **2005**, *4*, 864–868. (e) Kim, Y.; Cook, S.; Tuladhar, S. M.; Choulis, S. A.; Nelson, J.; Durrant, J. R.; Bradley, D. D. C.; Giles, M.; McCulloch, I.; Ha, C. S.; Ree, M. *Nat. Mater.* **2006**, *5*, 197–203.

(5) Brabec, C.; Zerza, G.; Cerullo, G.; De Silvestri, S.; Luzatti, S.; Hummelen, J. C.; Sariciftci, N. S. *Chem. Phys. Lett.* **2001**, *340*, 232–236.

(6) (a) Arkhipov, V. I.; Bässler, H. *Phys. Stat. Sol. A* **2004**, *201*, 1152–1187. (b) Peumans, P.; Forrest, S. R. *Chem. Phys. Lett.* **2004**, *398*, 27–31. (c) Offermans, T.; Meskers, S. C. J.; Janssen, R. A. J. *Chem. Phys.* **2005**, *308*, 125–133. (d) Müller, J. G.; Lupton, J. M.; Feldmann, J.; Lemmer, U.; Scharber, M. C.; Sariciftci, N. S.; Brabec, C. J.; Scherf, U. *Phys. Rev. B* **2005**, *72*, 195208. (e) Blom, P. W. M.; Mihailetchi, V. D.; Koster, L. J. A.; Markov, D. E. *Adv. Mater.* **2007**, *19*, 1551–1566.

(7) Braun, C. L. *J. Chem. Phys.* **1984**, *80*, 4157–4161.

(8) Mihailetchi, V. D.; Koster, L. J. A.; Hummelen, J. C.; Blom, P. W. M. *Phys. Rev. Lett.* **2004**, *93*, 216601.

(9) Mihailetchi, V. D.; Koster, L. J. A.; Blom, P. W. M.; Melzer, C.; De Boer, B.; Van Duren, J. K. J.; Janssen, R. A. J. *Adv. Funct. Mater.* **2005**, *15*, 795–801.

(10) Mihailetchi, V. D.; Xie, H.; De Boer, B.; Koster, L. J. A.; Blom, P. W. M. *Adv. Funct. Mater.* **2006**, *16*, 699–708.

(11) (a) Mandoc, M. M.; Veurman, W.; Koster, L. J. A.; De Boer, B.; Blom, P. W. M. *Adv. Funct. Mater.* **2007**, *17*, 2167–2173. (b) Mandoc, M. M.; Veurman, W.; Sweelssen, J.; Koetse, M. M.; Blom, P. W. M. *Appl. Phys. Lett.* **2007**, *91*, 073518.

(12) (a) Marsh, R. A.; Groves, C.; Greenham, N. C. *J. Appl. Phys.* **2007**, *101*, 083509. (b) Barker, J. A.; Ramsdale, C. M.; Greenham, N. C. *Phys. Rev. B* **2003**, *67*, 075205. (c) Watkins, P. K.; Walker, A. B.; Verschoor, G. L. B. *Nano Lett.* **2005**, *9*, 1814–1818.

(13) (a) Van Hal, P. A.; Janssen, R. A. J.; Lanzani, G.; Cerullo, G.; Zavelani-Rossi, M.; De Silvestri, S. *Phys. Rev. B.* **2001**, *64*, 075206. (b) Van Hal, P. A.; Janssen, R. A. J.; Lanzani, G.; Cerullo, G.; Zavelani-Rossi, M.; De Silvestri, S. *Chem. Phys. Lett.* **2001**, *345*, 33–38.

(14) (a) Montanari, I.; Nogueira, A. F.; Nelson, J.; Durrant, J. R.; Winder, C.; Loi, M. A.; Sariciftci, N. S.; Brabec, C. *Appl. Phys. Lett.* **2002**, *81*, 3001–3003. (b) Nogueira, A. F.; Montanari, I.; Nelson, J.; Durrant, J. R.; Winder, C.; Sariciftci, N. S. *J. Phys. Chem. B* **2003**, *107*, 1567–1573. (c) Offermans, T.; Meskers, S. C. J.; Janssen, R. A. J. *J. Chem. Phys.* **2003**, *119*, 10924–10929. (d) Kim, Y.; Cook, S.; Choulis, S. A.; Nelson, J.; Durrant, J. R.; Bradley, D. D. C. *Chem. Mater.* **2004**, *16*, 4812–4818. (e) Offermans, T.; Meskers, S. C. J.; Janssen, R. A. J. *Chem. Phys.* **2005**, *308*, 125–133.

(15) De, S.; Pascher, T.; Maiti, M.; Jespersen, K. G.; Kesti, T.; Zhang, F.; Inganäs, O.; Yartsev, A.; Sundström, V. *J. Am. Chem. Soc.* **2007**, *129*, 8466–8472.

(16) Offermans, T.; Meskers, S. C. J.; Janssen, R. A. J. *J. Appl. Phys.* **2006**, *100*, 074509.

(17) Van Duren, J. K. J.; Yang, X.; Loos, J.; Bulle-Lieuwma, C. W. T.; Sieval, A. B.; Hummelen, J. C.; Janssen, R. A. J. *Adv. Funct. Mater.* **2004**, *14*, 425–434.

(18) (a) Hoppe, H.; Sariciftci, N. S. *J. Mater. Chem.* **2006**, *16*, 45–61. (b) Yang, X.; Loos, J. *Macromolecules* **2007**, *40*, 1353–1362.

strong enhancement in device efficiency when going from 20 to 80 wt % PCBM has been explained by a surprising, yet very significant, 2 orders of magnitude increase in hole mobility (μ_h) at high PCBM concentration that was found when measuring hole-only devices in the dark. The increase coincides with the onset of phase separation.[9] Although this gives full understanding of the device performance, the effect of PCBM concentration and morphology on charge generation, has not been addressed.

One possibility to gain detailed insight into these issues, and possibly resolve the apparent discrepancies, is offered by materials that provide a charge transfer (CT) emission. CT emission is the radiative recombination of electrons and holes from a (photogenerated) charge separated state. Such an emissive charge separated state is often referred to as a CT state, as it is related to the ground-state by a charge transfer transition. CT emission has been observed in a few polymer:PCBM blends,[19–21] and a number of polymer:polymer blends.[22,23] In such blends, CT emission is sometimes referred to as exciplex emission when the corresponding CT absorption is not observed or hidden, however an exciplex is defined as an electronically excited complex of definite stoichiometry, "nonbonding" in the ground state. The decay time of this CT (or exciplex-like) emission is typically a few, or a few tens of nanoseconds, but, notably, does not extend into the microsecond regime. For example, for MDMO-PPV:PCNEPV blends the CT (exciplex) emission was $\tau_F = 1.6$ ns,[23] that is, more than 6 orders of magnitude shorter than the value that emerged from fitting the $J-V$ curve ($\tau_F =$ 10 ms).[11]

Until recently, most materials combinations that exhibit CT emission did not provide very efficient solar cells. One noticeable exception, however, is the type of blends of poly[2,7-(9,9-dialkylfluorene)-*alt*-5,5-(4′,7′-di-2-thienyl-2′,1′,3′-benzothiadiazole)] (PF*n*TBT, *n* being the number of carbons of the alkyl substituents, Figure 1) with PCBM for which both efficient photovoltaic devices,[24–28] and CT emission have been described.[21] PF10TBT:PCBM (1:4 by wt.) blends reach an AM 1.5 power conversion efficiency of $\eta = 4.2\%$, owing to a favorable high open-circuit voltage ($V_{OC} = 999$ mV) and internal quantum efficiency (IQE = 75%).[25,28] Transient absorption measurements on PF8TBT:PCBM blends have revealed a fast (~0.2 ps) charge transfer process, followed by charge separation of CT states into free charge carriers (~30 ps), and geminate charge recombination of free charge carriers on a ~30 ns time scale.[15,29]

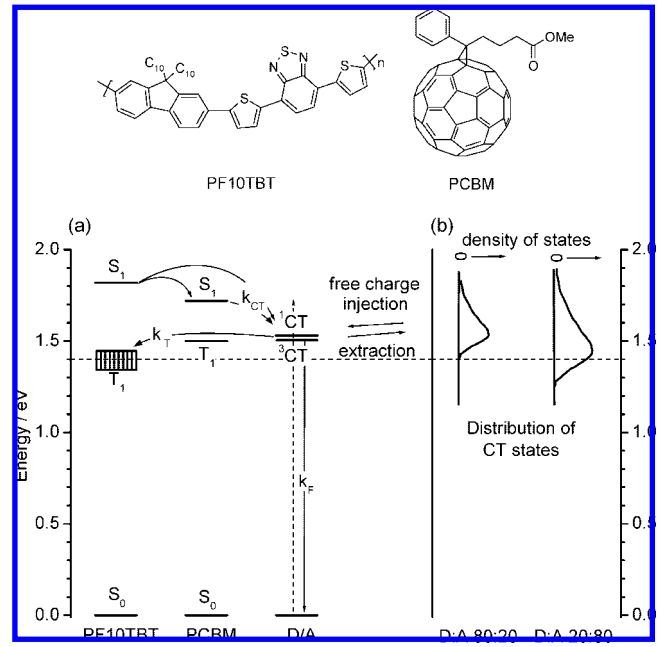

Figure 1. Chemical structures of PF10TBT and PCBM (top). (a) Jablonski diagram showing the singlet and triplet excited-state energies of PF10TBT and PCBM, and the CT state, relative to their ground states. The dashed arrow represents absorption from a ground-state D/A complex. The CT state can also be populated from S_1 states of PF10TBT or PCBM by charge transfer (k_{CT}). (b) Schematic energetic distribution of the CT states for two different PF10TBT:PCBM ratios, based on the results described in this work.

Here we present a comprehensive study of the CT emission with (time-resolved) photoluminescence of different PF10TBT:PCBM blends in films and in solar cell devices to investigate the kinetics, field dependence, and composition dependence of the electron−hole dissociation process. We find that the presence of PCBM clusters in films with high PCBM content strongly influences the photophysical properties. First, the higher relative permittivity (ε_r) of PCBM compared to PF10TBT causes the energy of the CT state (E_{CT}) and the V_{OC} to be lowered with increasing PCBM concentration. Second, the average decay time of the relatively short-lived ($<\tau>$ = ca. 4 ns) CT emission is further reduced with increasing PCBM concentration or by the application of an electric field. Using the Onsager−Braun model of geminate recombination we relate the field- and concentration-induced dissociation of the bound electron−hole pairs to the presence of larger crystalline domains of PCBM at high fullerene loading. A high electron mobility inside these clusters enables the dissociation of the CT excitons, despite their short lifetime.

(19) (a) Hasharoni, K.; Keshavarz-K, M.; Sastre, A.; Gonzalez, R.; Bellavia-Lund, C.; Greenwald, Y. *J. Chem. Phys.* **1997**, *107*, 2308–2312. (b) Kim, H.; Kim, J. Y.; Park, S. H.; Lee, K.; Jin, Y.; Kim, J.; Suh, H. *Appl. Phys. Lett.* **2005**, *86*, 183502.
(20) Benson-Smith, J. J.; Goris, L.; Vandewal, K.; Haenen, K.; Manca, J. V.; Vanderzande, D.; Bradley, D. D. C.; Nelson, J. *Adv. Funct. Mater.* **2007**, *17*, 451–457.
(21) Loi, M. A.; Toffanin, S.; Muccini, M.; Forster, M.; Scherf, U.; Scharber, M. *Adv. Funct. Mater.* **2007**, *17*, 2111–2116.
(22) (a) Alam, M. M.; Jenekhe, S. A. *J. Phys. Chem. B* **2001**, *105*, 2479–2482. (b) Zhang, X. J.; Kale, D. M.; Jenekhe, S. A. *Macromolecules* **2002**, *35*, 382–393. (c) Morteani, A. C.; Dhoot, A. S.; Kim, J.-S.; Silva, C.; Greenham, N. C.; Murphy, C.; Moons, E.; Ciná, S.; Burroughes, J. H.; Friend, R. H. *Adv. Mater.* **2003**, *15*, 1708–1712. (d) Morteani, A. C.; Sreearunothai, P.; Herz, L. M.; Friend, R. H.; Silva, C. *Phys. Rev. Lett.* **2004**, *92*, 247402. (e) Kietzke, T.; Neher, D.; Hörhold, H.-H. *Chem. Mater.* **2005**, *17*, 6532–6537. (f) Chasteen, S. V.; Haerter, J. O.; Rumbles, G.; Scott, J. C.; Nakazawa, Y.; Jones, M.; Hörhold, H.-H.; Tillmann, H.; Carter, S. A. *J. Appl. Phys.* **2006**, *99*, 033709. (g) Yin, C.; Kietzke, T.; Neher, D.; Hörhold, H.-H. *Appl. Phys. Lett.* **2007**, *90*, 092117.
(23) Offermans, T.; Van Hal, P. A.; Meskers, S. C. J.; Koetse, M. M.; Janssen, R. A. J. *Phys. Rev. B* **2005**, *72*, 045213.
(24) (a) Svensson, M.; Zhang, F.; Veenstra, S. C.; Verhees, W. J. H.; Hummelen, J. C.; Kroon, J. M.; Inganäs, O.; Andersson, M. R. *Adv. Mater.* **2003**, *15*, 988–991. (b) Zhang, F.; Jespersen, K. G.; Björström, C.; Svensson, M.; Andersson, M. R.; Sundström, V.; Magnusson, K.; Moons, E.; Yartsev, A.; Inganäs, O. *Adv. Funct. Mater.* **2006**, *16*, 667–674.
(25) Moet, D. J. D.; Slooff, L. H.; Kroon, J. M.; Chevtchenko, S. S.; Loos, J.; Koetse, M. M.; Sweelssen, J.; Veenstra, S. C. *Mater. Res. Soc. Symp. Proc.* **2007**, *974*, 0974-CC03-09.
(26) Jespersen, K. G.; Zhang, F.; Gadisa, A.; Sundström, V.; Yartsev, A.; Inganäs, O. *Org. Electron.* **2006**, *7*, 235–242.
(27) Andersson, L. M.; Zhang, F.; Inganäs, O. *Appl. Phys. Lett.* **2007**, *91*, 071108.
(28) Slooff, L. H.; Veenstra, S. C.; Kroon, J. M.; Moet, D. J. D.; Sweelssen, J.; Koetse, M. M. *Appl. Phys. Lett.* **2007**, *90*, 143506.
(29) De, S.;Kesti, T.;Maiti, M.;Zhang, F.;Inganäs, O.;Yartsev, A.;Pascher, T.;Sundström, V. *Chem. Phys.,* published online December, 8, 2007, doi:10.1016/j.chemphys.2007.11.018.

We argue that the presence of nanocrystalline domains is important for the performance of polymer solar cells by allowing dissociation of CT excited states.

II. Experimental Section

The preparation of PF10TBT (M_w = 34.9 kg/mol, PDI = 3.6) has been described previously.[25] In this study we employed the same batch that was formerly used to make η = 4.2% cells,[28] PCBM was obtained from Solenne BV.

Sample Preparation for Optical Spectroscopy. Thin (100−200 nm) films for UV−vis absorption, steady state and time-resolved photoluminescence (PL and TR-PL), and photoinduced absorption (PIA) were spin cast from chlorobenzene on quartz substrates. Typical solutions contained 1.0 wt % of material for preparing pristine PF10TBT films and 1−2 wt % total concentration for composite films. The solutions were stirred at 85 °C for at least 1 h prior to spin coating. The film thickness was determined by profilometry (Tencor P-10).

Preparation of Photovoltaic Devices and Light-Emitting Diodes. Glass substrates with patterned indium tin oxide (ITO) were cleaned by scrubbing with a soap solution, followed by ultrasonic treatments using acetone and isopropanol. Then, the glass/ITO substrates were treated in a UV/O_3 photoreactor. Poly[3,4-ethylenedioxythiophene]:poly[styrenesulfonate] (PEDOT:PSS, dispersion in water, HC Starck electronic grade Baytron P VP AI4083), filtered through a 5.0 μm hydrophilic PVDF filter, was applied by spin coating. The resulting PEDOT:PSS layers (50 nm) were annealed at 200 °C during 2 min. Layers of PF10TBT, with or without PCBM (135−220 nm) were spin coated from hot solutions in chlorobenzene on top of the PEDOT:PSS layer. A LiF(1.2 nm)/Al(80 nm) metal electrode was applied by evaporation through a shadow mask in a vacuum evaporator (10^{-5} mbar) that was placed in a glovebox filled with nitrogen ([O_2],[H_2O] < 1 ppm).

Sample Preparation and Characterization by AFM and TEM. Thin films (50−90 nm) of PF10TBT:PCBM blends were cast on a PEDOT:PSS layer (50 nm) from hot solutions of 0.8−1.2 wt % total concentration. Atomic force microscopy (AFM) measurements were performed under ambient conditions on a Digital Instruments Dimension 3100 with Nanoscope IIIa controller. NT-MDT NSG10 (force constant typically 11.5 N/m) cantilevers were used in tapping mode measurements. All measurements are repeated with different scan parameters and on several spots on the same sample to warrant reproducibility and to exclude scan artifacts.

For transmission electron microscopy (TEM) measurements the PF10TBT:PCBM layers were floated onto the surface of deionized water, and finally picked up by a 400 mesh copper grid. The bright-field morphology observation and selected area electron diffraction (SAED) measurements were conducted on a TECNAI G^2 20 transmission electron microscope (FEI Co, The Netherlands) operated at 200 kV. For SAED the instrument was calibrated with the diffraction pattern of gold.

Absorption and Photoluminescence Measurements. UV−vis absorption and steady state PL spectra were recorded with a Perkin-Elmer Lambda 900 spectrometer and an Edinburgh Instruments FS920 double-monochromator luminescence spectrometer using a Peltier-cooled red-sensitive photomultiplier, respectively. The fluorescence spectra were corrected for the optical density of the sample at the excitation wavelength, and for the detection sensitivity of the photomultiplier. Time-correlated single photon counting fluorescence studies were performed on an Edinburgh Instruments LifeSpec-PS spectrometer by photoexcitation with a 400 nm picosecond laser (PicoQuant PDL 800B) operated at 2.5 MHz and detection with a Peltier-cooled Hamamatsu microchannel plate photomultiplier (R3809U-50). Each intensity decay curve was fitted by a multiexponential fit by reconvolution of the instrument response function (IRF) using

$$I(t) = \int_{-\infty}^{t} IRF(t') \sum_{i=1}^{n} A_i \exp\left(-\frac{t-t'}{\tau_i}\right) dt'$$

where A_i is the amplitude of the i^{th} component with a lifetime τ_i. The decay parameters were recovered using the software package FluoFit version 4.1 supplied by PicoQuant GmbH, implementing the "nonlinear least-squares" method. The lifetime weighted fractional amplitude α_i corresponding to the lifetimes τ_i is given by $\alpha_i = (A_i\tau_i)/(\sum_i A_i\tau_i)$. Note that for the determination of α_i only positive values of A_i (corresponding to decay times) are taken into account.

Photoinduced Absorption. Near steady-state photoinduced absorption (PIA) spectra were recorded between 0.35 and 2.5 eV by excitation at 514 nm (2.41 eV) with a mechanically modulated (275 Hz) cw argon ion laser pump beam and by measuring the change in transmission of a tungsten-halogen probe beam through the sample (ΔT) with a phase sensitive lock-in amplifier after dispersion with a monochromator and detection using Si, InGaAs, and cooled InSb detectors. The pump power was typically 25 mW with a beam diameter of 2 mm. The PIA signal ($-\Delta T/T$) was corrected for the photoluminescence, which was recorded in a separate experiment. Samples were held at either 80 or 290 K in an inert nitrogen atmosphere using an Oxford Optistat continuous flow cryostat.

Electrochemistry. Cyclic voltammograms were recorded in an inert atmosphere with 0.1 M tetrabutylammonium hexafluorophosphate ($TBAPF_6$) in *o*-dichlorobenzene as supporting electrolyte. The working electrode was a platinum disk (0.2 cm^2) and the counter-electrode was a platinum electrode. Three different scan speeds were used for all compounds (10, 50, and 100 mV/s) using a Ag/AgCl reference electrode with the ferrocene/ferrocenium couple (Fc/Fc^+) as an internal standard (+0.41 eV vs Ag/AgCl in *o*-dichlorobenzene) and using a μAutolab II with a PGSTAT30 potentiostat.

Electroluminescence. This was characterized by a low-noise single-channel DC power source that can act as a voltage source or current source and as a voltage meter or current meter (Keithley 2400, Keithley Instruments). In a typical characterization of an LED the voltage is increased stepwise from −2.0 to +5.0 V, and back. Light from the diode is coupled into a silicon photodiode with photopic filter (Hamamatsu S9219) and read out by a current meter (Keithley 2400). Calibration of the photodiode was performed with a luminance meter (Minolta LS-110). For recording the electroluminescence spectra a fiber-coupled spectrograph (Avantes USB-2000) was used. The spectrometer was calibrated in wavelength and intensity. We define a positive bias voltage as the PEDOT:PSS electrode being charged positive with respect to the Al/LiF such that electrons, from Al/LiF and holes, from PEDOT:PSS can be injected.

Photovoltaic Characterization. Current−voltage characteristics were measured with a Keithley 2400 source measurement unit. Illumination was carried out with UV (GG 385) and infrared (KG1) filtered light from an uncalibrated tungsten halogen lamp (~75 mW/cm^2). The mismatch factor of this lamp to the AM1.5 (100 mW/cm^2) spectrum was not determined for the PF10TBT:PCBM devices.

III. Results and Discussion

A. Solar Cell Performance at Different Compositions. The $J-V$ characteristics of PF10TBT:PCBM devices containing 0, 5, 20, and 80 wt % PCBM recorded under white light illumination reveal clear trends with increasing PCBM concentration (Table 1, Figure 2). First, the open-circuit voltage (V_{OC}) decreases from 1.44 V for the device without PCBM to 1.15, 1.08, and 1.00 V for those containing 5, 20, and 80 wt % PCBM. Second, the short-circuit current density (J_{SC}), and the fill factor (FF) strongly increase with fullerene loading, resulting in a doubling of the estimated efficiency (η) when increasing the

Table 1. Active Layer Thickness (d), and $J-V$ Characteristics of PF10TBT:PCBM Devices Containing Different Amounts of PCBM

wt % PCBM	d (nm)	V_{OC} (V)	J_{SC} (mA cm^{-2})	FF	η^a (%)
0	135	1.44	0.033	0.29	0.014
5	135	1.15	0.12	0.24	0.034
20	220	1.08	5.26	0.32	1.85
50[b]	80−115	1.05−1.08	5.0−7.5	0.34−0.38	1.8−3.0
67[b]	125−170	1.01−1.03	7.1−8.1	0.42−0.49	3.4−3.7
80[b]	110−236	0.99−1.01	6.5−9.0	0.50−0.61	3.7−4.6
80	210	1.00	8.08	0.49	3.95

[a] Estimated efficiency; not corrected for the lamp spectrum. [b] From ref 25.

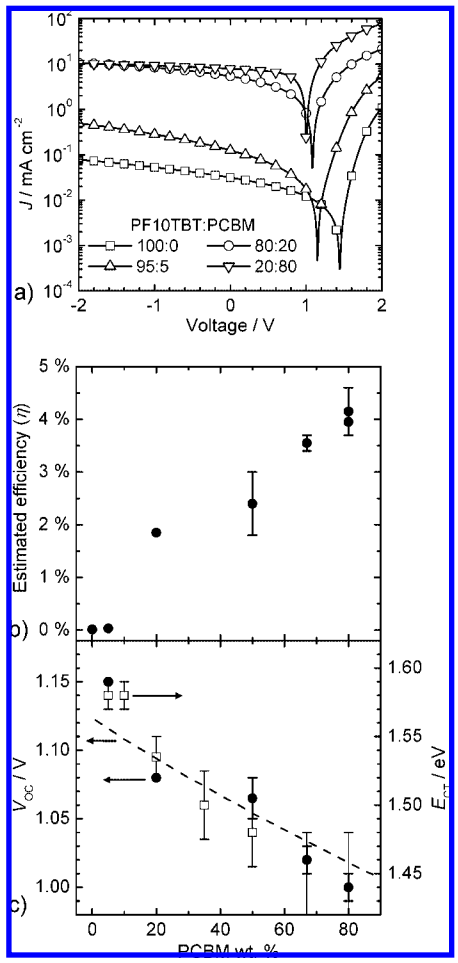

Figure 2. (a) $J-V$ curves of PF10TBT:PCBM photovoltaic devices for different compositions recorded under white light illumination. (b) Estimated efficiency (η, top), and (c) open-circuit voltage (V_{OC}, bottom, left axis), and the energy of the CT state (E_{CT}, bottom, right axis) as determined from the maximum CT emission (Figure 4d) vs PCBM concentration. For η and V_{OC} the data points with error bars are taken from ref 25. The dashed line shows the result of eq 2 for V_{OC}, using $r^+ = 4.5$ Å, $r^- = 5.6$ Å, and $\Delta = 0.81$ eV.

PCBM concentration from 20 to 80 wt %. The device containing 20 wt % PCBM absorbs more white light than that with 80 wt % PCBM, because of the strong absorption by PF10TBT in the visible range, explaining why at high reverse bias ($V < -1.85$ V) the photocurrent of the 20 wt % device is actually slightly higher than that of the 80 wt % device. De et al. recently reported on concentration-dependent transient absorption studies of blends of PF8TBT and PCBM on the subpicosecond time scale.[15,29] They concluded that at PCBM concentrations of 20 wt % and above, charge carriers are quantitatively formed upon photoexcitation, in accordance with this result. The higher J_{SC} for the 80 wt % device therefore results from a higher collection efficiency at short-circuit. Our device data can be directly compared to those reported by Moet et al. on the same PF10TBT:PCBM blends with intermediate PCBM concentrations (50, 67, and 80 wt % PCBM in Table 1, Figure 2b,c).[25] Even though different illumination setups were used, which may in particular have its influence on J_{SC} (and thus on η), the results follow the same trend. For PF8TBT:PCBM blends similar effects of the PCBM concentration on device performance were recently reported.[26,27]

In summary, the increases in J_{SC} and FF with PCBM concentration result in a strongly increased photovoltaic performance at 80 wt % PCBM. Concomitantly, a small but distinct, reduction in V_{OC} is observed.

B. Blend Morphology at Different Compositions. Thin free-standing films (50−90 nm) of PF10TBT:PCBM blends (0, 10, 20, 50, 80, and 100 wt % PCBM) were investigated with transmission electron microscopy (TEM). Bright-field TEM images shown in Figure 3a−c for the 20, 50, and 80 wt % PCBM films show that no significant phase separation is discernible for PF10TBT:PCBM ratios up to 50 wt % PCBM. For the highest PCBM concentration (80 wt %, Figure 3c) darker regions of 50−100 nm in diameter appear in a brighter background. In agreement with previous studies the darker regions are attributed to nanocrystalline PCBM domains that have a higher density than the polymer and appear at higher PCBM concentrations.[17,30] Selected area electron diffraction (SAED, Figure 3d) of PF10TBT films reveals some ordering as evidenced from a diffuse diffraction ring corresponding to a d-spacing of 4.9 Å, tentatively ascribed to a $\pi-\pi$ stacking distance. For nanocrystalline PCBM films d is 3.1 and 4.6 Å (Figure 3i).[31] For PF10TBT:PCBM blends (10−80 wt % PCBM, Figure 3e−h) the SAED is composed of the PF10TBT and PCBM Debye−Scherrer rings. Although below 50 wt % PCBM the rings are of low intensity; there is still ordering of both phases, even at lower PCBM concentration.

Atomic force microscopy (AFM) (Figure 3j−l) on the same blends revealed very smooth surfaces with root-mean-square roughness values of $R_{rms} = 0.47-0.72$ nm, measured at an area of 1×1 μm^2. The film containing 80 wt % PCBM showed height variations (~3.0 nm) that were much larger than for the other films (~1.0 nm). The height profile of the film containing 80 wt % PCBM showed comparable sizes (50−100 nm in diameter) as were found by TEM (compare Figure 3c and 3l).

In summary, the AFM and TEM measurements demonstrate that nanoscale (>10 nm) phase separation occurs at high fullerene concentration and results in 50−100 nm sized PCBM clusters at 80 wt % PCBM for PF10TBT:PCBM films spin cast from chlorobenzene. SAED measurements indicate the presence of nanocrystalline PCBM clusters also for lower concentrations that do not show up in the bright field TEM image. Overall the phase separation in PF10TBT:PCBM blends is very similar to that observed for MDMO-PPV:PCBM blends.[17,18]

C. CT Absorption and Emission of PF10TBT:PCBM Blends. The ground-state absorption spectrum of PF10TBT reveals two bands, with maxima at about 400 and 560 nm.

(30) Yang, X.; Loos, J.; Veenstra, S. C.; Verhees, W. J. H.; Wienk, M. M.; Kroon, J. M.; Michels, M. A. J.; Janssen, R. A. J. *Nano Lett.* **2005**, *5*, 579–583.
(31) Yang, X.; Van Duren, J. K. J.; Rispens, M. T.; Hummelen, J. C.; Janssen, R. A. J.; Michels, M. A. J.; Loos, J. *Adv. Mater.* **2004**, *16*, 802–806.

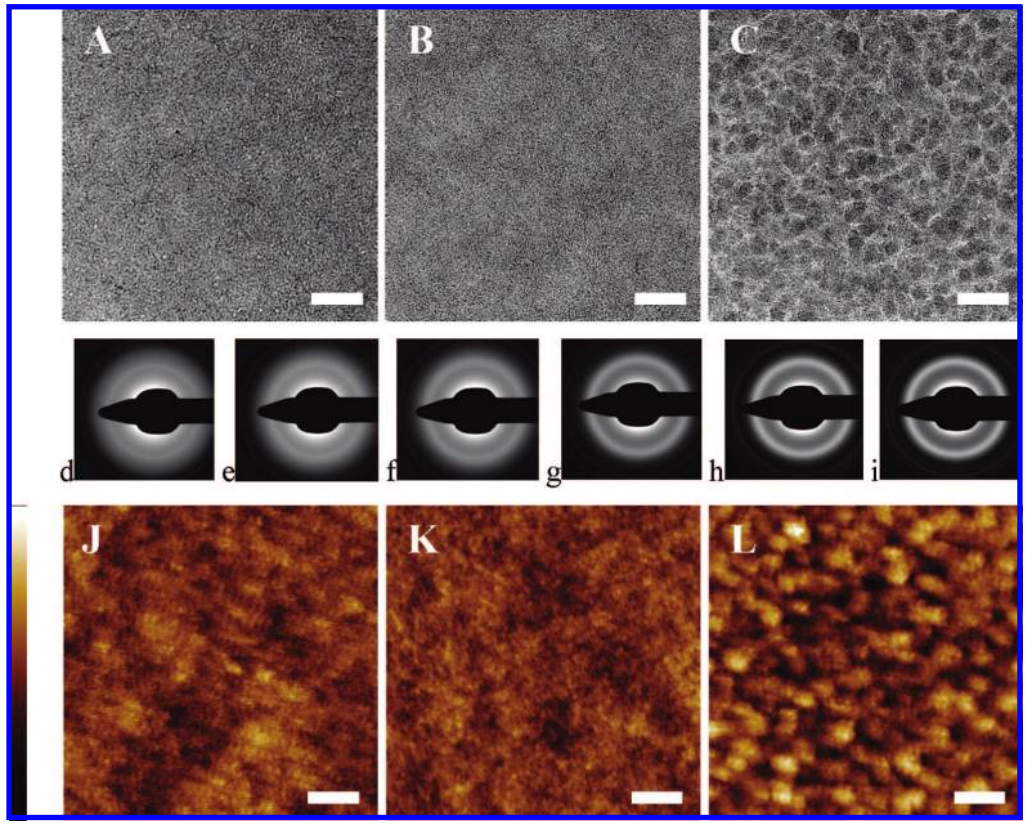

Figure 3. TEM (a−c) and AFM height (j−l) images of PF10TBT:PCBM films containing 20 (a and j), 50 (b and k), and 80 (c and l) wt % PCBM. The size of each image is width × height = 1.25 × 1.25 μm^2, the horizontal scale bar in images a−c and j−l is 200 nm and the vertical range of graphs j−l is 6 nm. Panels d−i show the SAED patterns of PF10TBT films containing 0, 10, 20, 50, 80, and 100 wt % PCBM, respectively.

Photoexcitation of a PF10TBT film at 560 nm results in a broad photoluminescence (PL) band with a maximum centered at 660−680 nm (Figure 4a). The PL emission intensity of PF10TBT (λ_{exc} = 400 or 560 nm, λ_{em} = 680 nm) is reduced by more than 2 orders of magnitude upon addition of only 10 wt % PCBM (Supporting Information, Figure S2). Recently De et al.[15] and Loi et al.[21] also reported such strong PL quenching for PF8TBT:PCBM blends. The strong PL quenching can be explained by rapid energy or electron transfer to PCBM. Next to the quenching of PF10TBT emission, photoexcitation of the PF10TBT:PCBM blends also reveals a broad, red-shifted emission between 700 and more than 840 nm (Figure 4c). After correcting for the residual PF10TBT emission, a broad band with a maximum at about 785 nm is obtained for the 10 wt % blend (Figure 4d). This emission does not originate from PCBM having an emission maximum at 720 nm with a shoulder around 800 nm for a thin film (Figure 4b). We attribute the broad and red-shifted luminescence to CT emission from a singlet CT state. In first approximation, this emission involves a transition of an electron from the LUMO (lowest unoccupied molecular orbital) of PCBM to the HOMO (highest occupied molecular orbital) of PF10TBT:PCBM. Loi et al.[21] observed similar emission characteristics for a PF8TBT:PCBM blend and also attributed it to emission of CT excitons. The CT state is *primarily* formed via photoexcitation of PF10TBT or PCBM in a very fast (∼ps) electron transfer reaction from PF10TBT to PCBM that effectively quenches the PL of the two components (k_{CT} in Figure 1a). As we will show in the following, the CT state can also be formed by direct excitation in a weak CT absorption band or via recombination of free electrons and holes (section D). The low overall intensity of the PL at 785 nm suggests that the intrinsic quantum yield of CT emission is low and that this state also decays nonradiatively to the ground state.

Time-resolved photoluminescence (TR-PL) measurements have been performed for PF10TBT:PCBM blends (0, 10, 20, 80, and 100 wt % PCBM) (Figure 5). For pristine PF10TBT, global analysis of multiple wavelength decay traces reveals two decay times. The major decay component, τ_1 = 1.17 ns, accounts for about 90% of the emission (Figure 5, Figure S3, Table S1). When 10 wt % PCBM is added to the film the PL lifetime of the PF10TBT singlet excited state (selectively probed at 670 nm) is strongly reduced. The decay time is shorter than the response time of our setup (τ_1 < 50 ps, Figure 5a). This is in good agreement with the steady state PL results because quenching of the polymer emission by more than 2 orders of magnitude implies a PL decay time $\tau < \tau_1$(PF10TBT)/100 = 12 ps. The PL decay recorded at 710 and 780 nm, where predominantly PCBM and CT emission are probed (Figure 5b and 5c), were fitted to an exponential decay with three components (Table 2). Again, the shortest PL decay time, arising from residual PF10TBT emission, was too short to be accurately determined and was fixed at τ_1 = 25 ps, while the other two decay components were free parameters. Selecting a shorter τ_1 has only a minor influence on the magnitudes of τ_2 and τ_3, and their relative amplitudes. For the 10 wt % blend, relatively short (τ_2 = 0.5 ns) and relatively long (τ_3 = 3−4 ns) decay components were found with lifetime weighted fractional intensities, α_i, that are a factor of 3−9 larger for the longer component (Table 2). The longest decay component (τ_3 = 3.94 ns at 780 nm) is actually longer than the lifetime of the pristine materials (τ = 1.15 and 1.17 ns for PCBM and PF10TBT). Such increased decay times are typical for CT emission in blends of

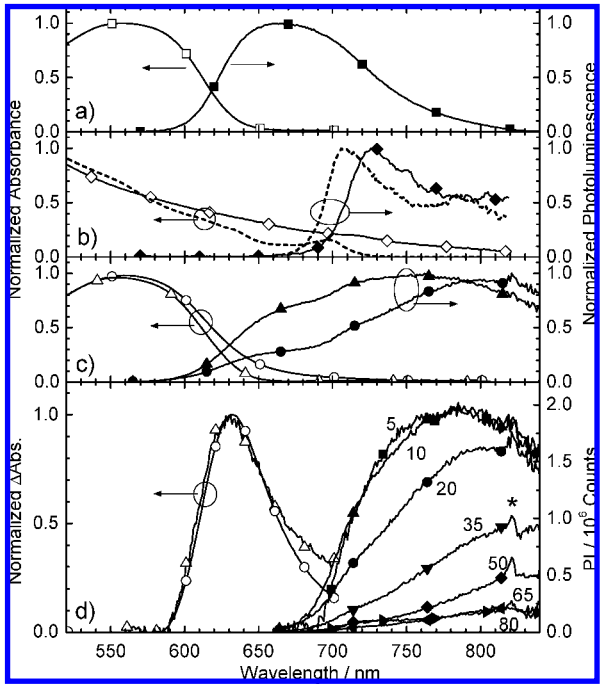

Figure 4. Normalized absorbance (left axis, open symbols) and photoluminescence (right axis, closed symbols) spectra of thin (a) PF10TBT (□,■), (b) PCBM (◇,♦), and (c) PF10TBT:PCBM 90:10 (Δ,▲) and 80:20 (○,●) blend films. The dashed lines in panel b are the PCBM absorbance and photoluminescence spectra in *o*-dichlorobenzene solution. Panel d shows the normalized differential absorbance (ΔAbs) spectra of PF10TBT:PCBM blends containing 10 (Δ) and 20 (○) wt % PCBM compared to films of the pristine materials (left axis), and photoluminescence spectra of blends containing 5−80 wt % PCBM corrected for the PF10TBT rest emission, and the amount of photons absorbed at the excitation wavelength (λ_{exc} = 560 nm, right axis). The feature at 820 nm (∗) is an artifact that was also observed for a clean quartz plate.

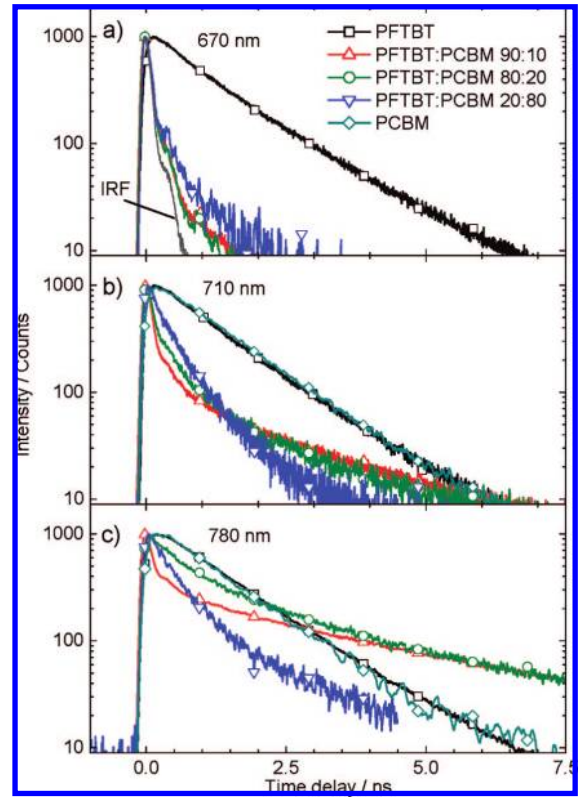

Figure 5. Time-resolved photoluminescence of PF10TBT:PCBM blends and pristine PF10TBT and PCBM films on quartz, probed at 670 nm (a), 710 nm (b), and 780 nm (c). The thin solid line in panel a is the instrument response function (IRF). All films were excited at 400 nm.

conjugated polymers.[22,23] Loi et al. reported decay times of τ_1 = 0.32 ns and τ_2 = 3.1 ns to describe the PL decay of a PF8TBT:PCBM 33:67 blend at 820 nm.[21]

The multiexponential character of the CT emission decay could result from a distribution of CT states with different electron−hole distances or from an equilibrium between charge carrier dissociation and recombination. The longer decay times at longer wavelength (compare 780 and 710 nm in Table 2) point to a relaxation of CT states to lower energy with time. However, a contribution from the decay of the (quenched, $\tau \leq$ 1.15 ns) PCBM singlet state at 710 nm cannot be excluded.

The longest lifetime component of the CT state of 1.5−4 ns that we find (Table 2), is somewhat shorter than the geminate recovery time of the ground state (∼30 ns) measured by De et al. for PF8TBT:PCBM.[15] This suggests that the recovery of the ground-state is also due to nonradiative recombination of free charges.

Comparison of the UV/vis absorption spectrum of the pristine PF10TBT film to those of the blend containing 10 wt % of PCBM (Figure 4) reveals only minor differences, even though the emission of the blend at 780 nm arises predominantly from CT emission (Figure 4c), demonstrating that the interaction between PF10TBT and PCBM in the ground-state is weak. However, in the wavelength region λ > 600 nm a slightly enhanced absorption is observed in the blend relative to the pristine film (Figure 4c). The difference spectrum (ΔOD) of the PF10TBT:PCBM 90:10 blend and pristine PF10TBT and PCBM films shows a clear band at 628 nm (1.97 eV) with a near Gaussian line shape (Figure 4d). This band was also observed in the differential photoluminescence excitation spectrum (Supporting Information, Figure S1), and its shape is typical for CT absorption observed for small molecule electron donor−acceptor combinations in solution.[32] The presence of a CT absorption band evidences a non-negligible interaction in the ground-state between PF10TBT and PCBM, as previously reported in other conjugated polymer:PCBM blends.[20,33] By blending the two materials, a different polymer interchain interaction could also cause changes in the absorption spectrum. However, the expected reduced interchain interactions upon blending would reduce the intensity at the red edge of the absorption band and lead to a negative differential absorption at λ > 600 rather that the positive band which is observed here.

In summary, upon photoexcitation the polymer emission of a PF10TBT:PCBM film with 10 wt % PCBM is strongly quenched compared to a pristine PF10TBT film, and a broad, longer-lived, red-shifted emission band appears, assigned to a CT transition. The corresponding CT absorption band can be observed in the differential absorption (and PL excitation) spectra. The CT emission arises from a state that is formed by charge transfer (k_{CT} in Figure 1) from a photoexcited singlet PF10TBT or PCBM state or by direct absorption from a PF10TBT:PCBM complex in the ground state (dashed arrow

(32) Zhou, J.; Findley, B. R.; Teslja, A.; Braun, C. L.; Sutin, N. *J. Phys. Chem. A* **2000**, *104*, 11512–11521.
(33) (a) Goris, L.; Poruba, A.; Hod'akova, L.; Vanecek, M.; Haenen, K.; Nesladek, M.; Wagner, P.; Vanderzande, D.; De Schepper, L.; Manca, J. V. *Appl. Phys. Lett.* **2006**, *88*, 052113. (b) Goris, L.; Haenen, K.; Nesladek, M.; Wagner, P.; Vanderzande, D.; De Schepper, L.; d'Haen, J.; Lutsen, L.; Manca, J. V. *J. Mater. Sci.* **2005**, *40*, 1413–1418.

Table 2. Analysis of TR-PL Decay Traces of PF10TBT:PCBM Blends

wt % PCBM	λ (nm)	τ_1 (ns)	α_1[a]	τ_2 (ns)	α_2[a]	τ_3 (ns)	α_3[a]	χ^2	$\langle\tau\rangle$[b] (ns)
10	710	0.025[c]	0.41	0.53	0.15	2.78	0.44	1.07	2.21
20	710	0.025[c]	0.47	0.42	0.25	2.26	0.28	0.86	1.39
80	710	0.025[c]	0.28	0.32	0.45	1.04	0.28	0.85	0.60
100	710	1.15	1.0					0.97	
10	780	0.025[c]	0.11	0.57	0.09	3.94	0.79	1.27	3.60
20	780	0.025[c]	0.06	0.58	0.25	2.98	0.69	1.04	2.34
80	780	0.025[c]	0.09	0.37	0.48	1.48	0.43	4.3[d]	0.89
100	780	1.15	1.0					8.8[d]	

[a] α_i is the lifetime weighted fractional intensity of each component. [b] The average lifetime of the longer decay times: $\langle\tau\rangle = (\alpha_2\tau_2+\alpha_3\tau_3)/(\alpha_2+\alpha_3)$. [c] The shortest decay time was fixed to $\tau_1 = 25$ ps for the fit of the other decay times, because it is shorter than the response time of our setup. [d] The large value of χ^2 is caused by the low signal intensity.

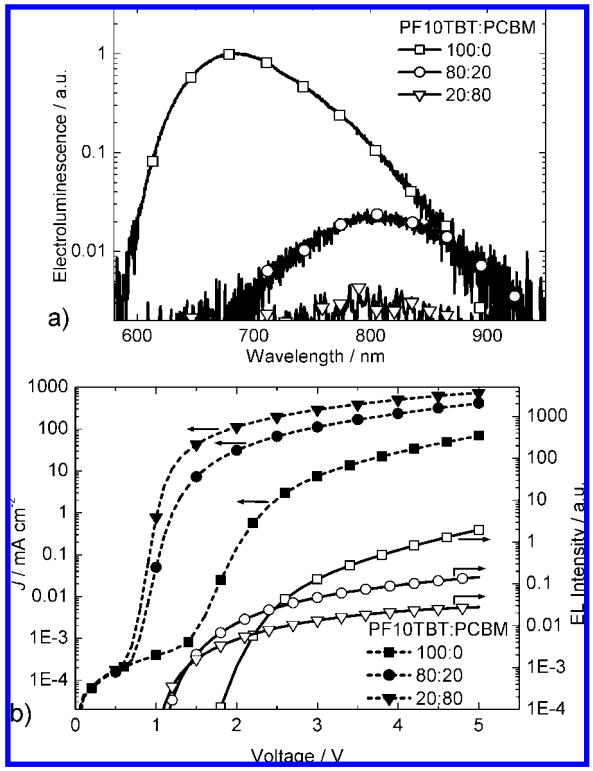

Figure 6. (a) Electroluminescence spectra of devices containing thin films of PF10TBT:PCBM blends with 0 (■), 20 (●), and 80 (▼) wt % PCBM. The operating voltage is +4 V and intensities are relative to the device containing only PF10TBT. (b) $J-$ (left axis) and light output-voltage (right axis) characteristics of the three devices.

in Figure 1). For a blend containing 10 wt % PCBM the optical density of the CT band at 628 nm is about a factor of 25 lower than that of PF10TBT at 560 nm, and the contribution of CT absorption to the total absorbance at 560 nm is less than 1%.

D. CT Emission in Electroluminescence. In addition to photoexcitation, CT emission can also be created by charge carrier injection. The electroluminescence (EL) of the (photovoltaic) devices containing 0, 20, and 80 wt % PCBM was measured and the results are shown in Figure 6. The steady state EL spectra (Figure 6a) recorded at +4 V bias resemble the PL spectra in Figure 4a and c. The device containing only PF10TBT shows a broad emission with a maximum at 685 ± 5 nm and the device containing 20 wt.% PCBM reveals a 50 × less intense, broad emission with a maximum at 800 nm. A distinct difference between the PL and EL spectra of the blends is the absence in the EL spectrum of any emission from either of the two separate components, demonstrating that in EL, PF10TBT and PCBM are not directly excited. Instead electrons, injected from the LiF/Al electrode into the LUMO of PCBM, and holes, injected from PEDOT:PSS into the HOMO of PF10TBT, recombine at the interface of the two materials, populating the intermolecular excited CT state.

Figure 6b shows the *J-V* and light output-voltage characteristics of the three devices. These plots show three important effects. First, the devices containing blends of PF10TBT and PCBM have an onset voltage for light output, $V_{on} = 1.13 \pm 0.04$ V, that is ca. 0.65 V lower than that of the device containing only PF10TBT ($V_{on} = 1.79$ V), and the onset matches with a sharp rise in current density. The lower V_{on} in the blends corresponds to an easier injection of electrons in the LUMO of PCBM ($E^\circ_{red} = -1.08$ V vs Fc/Fc^+) than in that of PF10TBT ($E^\circ_{red} = -1.62$ V vs Fc/Fc^+), showing that excited PF10TBT:PCBM CT states are created by hole and electron injection into the HOMO of PF10TBT and the LUMO of PCBM, respectively, without prior formation of excited PF10TBT. Second, V_{on} is lower for the film containing 80 wt % ($V_{on} = 1.09$ V) than for that containing 20 wt % of PCBM ($V_{on} = 1.17$ V), indicating that energetically lower states can be accessed in films with higher PCBM concentration. Third, Figure 6b shows that above 1.4 V the light output for the device containing 80 wt % PCBM is lower than that containing 20 wt %, while the current density is higher. This indicates less charge recombination or more nonradiative recombination in the 80 wt % device.

In summary, excited CT states can be formed by recombination of injected charge carriers in addition to photoexcitation. The onset voltage for carrier injection and light output in the PF10TBT:PCBM blend is less than in the pristine materials and is lowered with increasing PCBM concentration.

E. Effect of PCBM Concentration on CT Emission. Because the morphology of PF10TBT:PCBM blends changes considerably upon going from 20 to 80 wt % PCBM, it is of interest to study the optical properties of the different blend compositions. The intensity of the CT absorption band increases with the amount of PCBM added to the PF10TBT film, at least up to 50 wt %. This is in agreement with reports on other polymer:PCBM blends,[20,33b] and can be explained by the fact that more PF10TBT:PCBM contact pairs are present in films with higher PCBM concentration. Remarkably, while the CT absorption band does not change its position, the CT emission gradually shifts to the red with higher PCBM concentration (Figure 4d). The shift—from 785 nm (1.58 eV) at 5 and 10 wt %, via 810 nm (1.53 eV) for 20 wt %, to >840 nm (<1.48 eV) at 50 wt % and higher PCBM concentrations—indicates a reduction of the singlet excited CT state energy (E_{CT}). The lower E_{CT} can be explained by the higher relative permittivity of PCBM ($\varepsilon_r =$

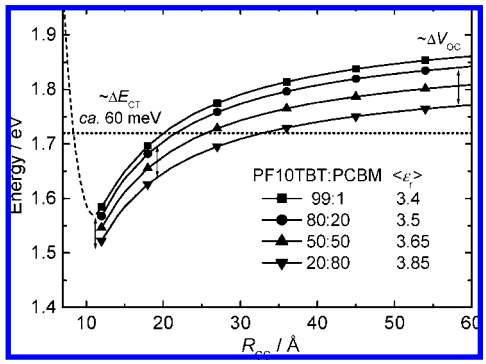

Figure 7. E_{CT} vs R_{CC} as determined from eq 1 for different spatially averaged relative permittivities, $<\varepsilon_r>$, representing different weight ratios of PF10TBT and PCBM (see legend). At short cation−anion distances (R_{CC} < 12 Å) a dashed line is added which tentatively takes into account the repulsion of cation and anion (see text). The dotted line indicates the PCBM S_1 energy.

4.0 ± 0.1)[34,35] than that of PF10TBT (ε_r = ca. 3.4),[36,37] as suggested by Loi et al.[21] We find $<\varepsilon_r>$ = 3.5 for 20 wt % and $<\varepsilon_r>$ = 3.85 for 80 wt % PCBM for the spatially averaged relative permittivities.[38] These values can be used to predict E_{CT}, by using the equation for the Gibbs free energy of photoinduced electron transfer:[39]

$$E_{CT} = \Delta_{ET}G^0 + E(S_1) = e[E^0(D/D^{+\bullet}) - E^0(A/A^{-\bullet})] - Z\left(\frac{1}{\varepsilon_{ref}} - \frac{1}{<\varepsilon_r>}\right)\left(\frac{1}{r^+} + \frac{1}{r^-}\right) - \frac{Z}{\varepsilon_r}\left(\frac{2}{R_{CC}}\right) \quad (1)$$

with $Z = e^2/(8\pi\varepsilon_0)$ and e and ε_0 the electron charge and the vacuum permittivity, respectively. For PCBM $E°(A/A^{-\bullet})$ = −1.08 V versus Fc/Fc^+ was obtained by cyclic voltammetry, while for PF10TBT the onset of oxidation, E^{onset} $(D/D^{+\bullet})$ = +0.30 V versus Fc/Fc^+ was found, both in *o*-dichlorobenzene (ε_{ref} = 9.93). The radius of the cation was set to r^+ = 4.5 Å, and that of the anion to r^- = 5.6 Å.[49a] In Figure 7 we have used these values to estimate E_{CT} as a function of $<\varepsilon_r>$ and the center-to-center cation−anion separation (R_{CC}) that seems reasonable for emissive CT states. At short R_{CC}, the energy will increase when radical cation and radical anion come within the sum of their van der Waals radii. This is tentatively represented by the dashed line in the graph for the 99:1 blend. From eq 1 we find a stabilization energy of 60 ± 20 meV for the film containing 80 versus that containing 20 wt % PCBM for R_{CC} = 10−20 Å, induced by the more polar medium given by PCBM. This corresponds to the observed >50 meV shift of the PL maximum. Although E_{CT} predicted with eq 1 is sensitive to the choice of the values for r^+ or R_{CC}, the stabilization energy, the difference between E_{CT} in 20 and 80 wt % PCBM mixtures, is nearly independent of r^+ or R_{CC}.

The reduction of V_{on} of EL by 70 meV (from 1.16 to 1.09 V, *vide supra*), and of V_{OC} by 80 meV (from 1.08 to 1.00 V) upon increasing the PCBM concentration from 20 to 80 wt % PCBM correlate with the red shift of the PL maximum of the CT emission (E_{CT} in Figure 2c), resulting in the apparent relation $V_{OC} = (1/e)(E_{CT} - 0.45 \pm 0.05$ eV). This observation indicates that not only the energy of bound electron−hole pairs, but also that of free charge carriers in the blend is reduced with increasing PCBM concentration, via its higher ε_r. The energy of free charge carriers may be estimated by eq 1, by taking $R_{CC} = \infty$. Hence, eq 2 can be used to describe the dependence of the V_{OC} on PCBM content by the average $<\varepsilon_r>$ of the blend (Figure 2c):

$$V_{OC} = [E^0(D/D^{+\bullet}) - E^0(A/A^{-\bullet})] - \frac{Z}{e}\left(\frac{1}{\varepsilon_{ref}} - \frac{1}{<\varepsilon_r>}\right)\left(\frac{1}{r^+} + \frac{1}{r^-}\right) - \Delta \quad (2)$$

It is generally observed that V_{OC} of organic photovoltaic devices is almost linearly dependent on the difference between the HOMO of the electron donating material and the LUMO of the electron accepting material,[40] and we add to this that the energetic positions of the HOMO and LUMO levels are dependent on ε_r. The Δ describes energetic losses of the charge pair after its dissociation and before entering the external electric circuit. One of the factors influencing Δ is band bending at the electrodes as a result of a build-up of charge carriers,[41] which can be dependent on PCBM concentration. However, by using a model presented by Kemerink et al.,[42] we find that only a minor influence of the PCBM concentration on the V_{OC} is expected (<0.025 V) between 20 and 80 wt % PCBM using a constant offset between the HOMO of the donor and the LUMO of the acceptor material, that is, excluding the second term in eq 2. This indicates that the influence of ε_r on the variation of V_{OC} is the major contributor in this concentration range.

Next to the wavelength shift of the maximum of the CT emission there is a strong drop in intensity by almost a factor of 10 upon increasing the PCBM concentration from 5−10 wt % to 65−80 wt % PCBM (Figure 4d). This reduction indicates the presence of an additional, competing nonradiative decay pathway for excited CT states at higher fullerene concentrations. Time-resolved photoluminescence measurements were carried out to elucidate the nature of this additional pathway. The analysis of the TR-PL data at 710 and 780 nm at high PCBM

(34) Mihailetchi, V. D.; Van Duren, J. K. J.; Blom, P. W. M.; Hummelen, J. C.; Janssen, R. A. J. *Adv. Funct. Mater.* **2003**, *13*, 43–46.
(35) De Haas, M. P.; Warman, J. M.; Anthopoulos, T. D.; De Leeuw, D. M. *Adv. Funct. Mater.* **2006**, *16*, 2274–2280.
(36) Persson, N.-K.; Arwin, H.; Inganäs, O. *J. Appl. Phys.* **2005**, *97*, 034503.
(37) The value of $\varepsilon_r = n^2 = 3.4$ is derived from the value of n = 1.85 for PF8TBT (ref 36) and PF10TBT (ref 28) when extrapolated to $\omega = 0$.
(38) If the densities of PF10TBT (ρ = ∼1.10 g cm^{-3}) and PCBM (ρ = 1.50 g cm^{-3}) are taken into account, ε_r (PF10TBT) = 3.4 and ε_r (PCBM) = 4.0 result in $<\varepsilon_r>$ = 3.5 (20 wt %) and $<\varepsilon_r>$ = 3.85 (80 wt % PCBM).
(39) (a) Weller, A. Z. *Phys. Chem. Neue Folge* **1982**, *133*, 93–98. (b) Oevering, H.; Paddon-Row, M. N.; Heppener, M.; Oliver, A. M.; Cotsaris, E.; Verhoeven, J. W.; Hush, N. S. *J. Am. Chem. Soc.* **1987**, *109*, 3258–3269. (c) Kroon, J.; Verhoeven, J. W.; Paddon-Row, M. N.; Oliver, A. M. *Angew. Chem., Int. Ed.* **1991**, *30*, 1358–1361.
(40) (a) Brabec, C. J.; Cravino, A.; Meissner, D.; Sariciftci, N. S.; Fromherz, T.; Rispens, M. T.; Sanchez, L.; Hummelen, J. C. *Adv. Funct. Mater.* **2001**, *11*, 374–379. (b) Gadisa, A.; Svensson, M.; Andersson, M. R.; Inganäs, O. *Appl. Phys. Lett.* **2004**, *84*, 1609–1611. (c) Veldman, D.; Offermans, T.; Sweelssen, J.; Koetse, M. M.; Meskers, S. C. J.; Janssen, R. A. J. *Thin Solid Films* **2006**, *511−512*, 333–337. (d) Cremer, J.; Bäuerle, P.; Wienk, M. M.; Janssen, R. A. J. *Chem. Mater.* **2006**, *18*, 5832–5834. (e) Roquet, S.; Cravino, A.; Leriche, P.; Alévéque, O.; Frère, P.; Roncali, J. *J. Am. Chem. Soc.* **2006**, *128*, 3459–3466. (f) Mutolo, K. L.; Mayo, E. I.; Rand, B. P.; Forrest, S. R.; Thompson, M. E. *J. Am. Chem. Soc.* **2006**, *128*, 8108–8109. (g) Scharber, M. C.; Mühlbacher, D.; Koppe, M.; Denk, P.; Waldauf, C.; Heeger, A. J.; Brabec, C. J. *Adv. Mater.* **2006**, *18*, 789–794. (h) Kooistra, F. B.; Knol, J.; Kastenberg, F.; Popescu, L. M.; Verhees, W. J. H.; Kroon, J. M.; Hummelen, J. C. *Org. Lett.* **2007**, *9*, 551–554. (i) Rand, B. P.; Burk, D. P.; Forrest, S. R. *Phys. Rev. B* **2007**, 115327. (j) Cravino, A. *Appl. Phys. Lett.* **2007**, *91*, 243502.
(41) Mihailetchi, V. D.; Blom, P. W. M.; Hummelen, J. C.; Rispens, M. T. *J. Appl. Phys.* **2003**, *94*, 6849.
(42) Kemerink, M.; Kramer, J. M.; Gommans, H. H. P.; Janssen, R. A. J. *Appl. Phys. Lett.* **2006**, *88*, 192108.

concentration (Figure 5) resulted in decay times with shorter decay components for both τ_2 and τ_3 (Table 2) than for the 10 wt % PCBM blend film. Furthermore the fractional intensity of the shorter decay component (τ_2) increases relative to that of the longer one (τ_3) with fullerene loading. The shorter decay time is consistent with the strongly reduced CT emission and supports the presence of an additional nonradiative decay pathway for CT states at higher PCBM concentration. A likely mechanism involves dissociation of CT states into electrons and holes with longer separation distance that do not recombine radiatively. The products of this dissociation can be investigated with photoinduced absorption measurements.

In summary, at higher PCBM concentration, the CT state shifts to lower energy as a result of the increased permittivity, also causing a reduction of V_{OC}. Additionally, with increasing PCBM concentration, the decay time of CT states is reduced via an additional nonradiative pathway.

F. Photoinduced Absorption of PF10TBT:PCBM Blends. The effect of increasing the amount of PCBM from 0 to 80 wt % in PF10TBT on the formation of long-lived excited states was further studied using near steady-state photoinduced absorption (PIA) measurements at $T = 290$ K (Figure 8). Photoexcitation of pristine PFnTBT films results in the formation of a triplet state that absorbs between ~1.1 and 1.9 eV with a maximum at ca. 1.5 eV.[43] Our attribution to a triplet−triplet (T_1-T_n) absorption is based on the similarity to the PIA characteristics of PF10TBT in dilute toluene solution, showing a 0.1 eV blue-shifted T_1-T_n absorption, with a lifetime of $\tau = 10$ μs that is reduced upon addition of triplet sensitizers, and can be sensitized via the PCBM triplet.[44,45] In the film, the lifetime of the PF10TBT triplet exciton is about 1 μs at 290 K.[46] Photoexcitation of the PF10TBT:PCBM blend containing 80 wt % PCBM, on the other hand, produces the PIA spectrum of the radical cation of PF10TBT that exhibits a strong band maximizing below 0.4 eV and a 2-fold weaker band at 1.25 eV, and has a decay time of $\tau = 25-30$ μs.[47] This long lifetime is associated with a minority population of trapped charge carriers that have escaped the much faster geminate recombination that occurs with a decay time on the order of ~30 ns.[15] The fullerene anion has a weak absorption band around 1.2 eV that only weakly contributes to the PIA spectra of polymer:fullerene blends and is likely superimposed on the 1.25 eV band.[48] For the 10 and 20 wt % blends the spectra are a superposition of the spectra of the PF10TBT triplet exciton and the PF10TBT radical cation. At these lower PCBM concentrations, the decay time of the PF10TBT radical cation is less than 10 μs (measured at 0.48 eV), and hence significantly shorter than for the 80 wt % PCBM blend. The decay time of the PF10TBT triplet could not be determined owing to the low signal intensity and the overlap with the absorption of the radical cation.

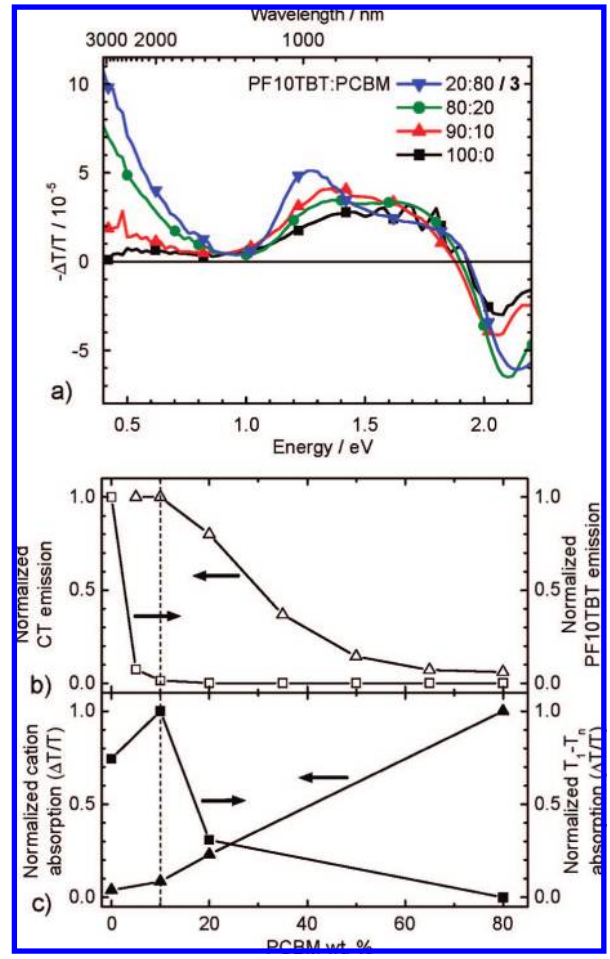

Figure 8. (a) PIA spectra recorded at 290 K of spin cast PF10TBT:PCBM thin films containing 0 (■), 10 (Δ), 20 (●), and 80 (▼) wt % PCBM, excited at $\lambda = 514$ nm. The spectra are corrected for the amount of photons absorbed at the excitation wavelength. The intensity of the 20:80 spectrum is divided by a factor of 3. The irregularities in the spectrum of the pristine PF10TBT film between 1.4 and 2.0 eV are a result of the high fluorescence intensity ($\Delta T/T = 6 \times 10^{-4}$ at 1.85 eV) relative to the PIA signal, such that the fluorescence correction is very sensitive to small fluctuations in the laser intensity. (b) Normalized intensities of the CT emission (Δ, left axis), and PF10TBT emission (□, right axis), and (c) normalized PF10TBT radical cation absorption at 0.5 eV (▲, left axis), and the PF10TBT T_1-T_n absorption at 1.35 eV (■, right axis) as a function of the PCBM concentration. The triplet absorption was corrected for that of the radical cation at 1.35 eV, assuming that PF10TBT triplet excitons are absent in the PF10TBT:PCBM 20:80 blend.[47] The lines are a guide to the eye.

(43) Wang, P.; Abrusci, A.; Wong, H. M. P.; Svensson, M.; Andersson, M. R.; Greenham, N. C. *Nano Lett.* **2006**, *6*, 1789–1793.

(44) In mixtures in toluene the triplet exciton of tetraphenylporphine (H2TPP, $E(T_1) = 1.43$ eV, ref 45) is in equilibrium with that of PF10TBT upon the addition of PF10TBT, whereas that of tetracene ($E(T_1) = 1.27$ eV, ref 45) quenches the triplet exciton of PF10TBT. We expect the energy of the PF10TBT triplet to change minimally upon going from solution to the solid state as the energetic position of the singlet exciton also hardly shifts (both in absorption and in emission).

(45) Monkman, A. P.; Burrows, H. D.; Da, G.; Miguel, M.; Hamblett, I.; Navaratnam, S. *Synth. Met.* **2001**, *116*, 75–79.

(46) At 80 K a decay time of $\tau = 10-15$ μs was determined for a thin film of PF10TBT over the full spectrum (see Supporting Information, Figure S5). At 290 K the decay time of the triplet exciton is within the time response of our setup; however, the 10-fold reduction in intensity infers a decay time of about 1 μs.

(47) There are two strong indications that the PF10TBT radical cation is the only significant contributor to the photoinduced absorption spectrum of the PF10TBT:PCBM 1:4 blend at 290 K: (1) an identical spectrum is found for a blend of PF10TBT with TCAQ (a stronger electron acceptor) at 290 K (Supporting Information, Figure S4), and (2) fits of the frequency dependence resulted in exactly the same lifetime ($\tau = 25-30$ μs) at 0.48, 1.30, and 1.70 eV. If the triplet absorption would substantially (>10%) contribute to the spectrum, the decay time at the high energy band would be shorter.

(48) (a) Smilowitz, L.; Sariciftci, N. S.; Wu, R.; Gettinger, C.; Heeger, A. J.; Wudl, F. *Phys. Rev. B* **1993**, *47*, 13835–13842. (b) Lee, K.; Janssen, R. A. J.; Sariciftci, N. S.; Heeger, A. J. *Phys. Rev. B* **1994**, *49*, 5781–5784. (c) Lee, K.; Miller, E. K.; Sariciftci, N. S.; Hummelen, J. C.; Wudl, F.; Heeger, A. J. *Phys. Rev. B* **1996**, *54*, 10525–10529. (d) Lies, M.; Vardeny, Z. V.; Lane, P. A. *Phys. Rev. B* **1999**, *59*, 11053–11061.

The PIA intensities of the PF10TBT radical cation (at 0.5 eV) and the triplet exciton (at 1.35 eV, and after correcting for the overlapping radical cation absorption) are compared to that of PF10TBT fluorescence and PF10TBT:PCBM CT emission in Figure 8b,c. We find that at 10 wt % PCBM the PF10TBT singlet emission is fully quenched, but that for the same film the intensity of the PF10TBT triplet absorption is even somewhat higher than that of the pristine PF10TBT film. This enhanced formation of triplet PF10TBT excitons under conditions where the PF10TBT singlet state is short-lived ($\tau < 12$ ps, *vide supra*) indicates that the triplet state is not formed via intersystem crossing from the singlet excited-state of the polymer. Instead, we propose that at 10 wt % PCBM, triplet excitons are efficiently formed via the CT state. Notably, at this PCBM concentration the CT state energy ($E_{CT} = 1.53$ eV) is well above the triplet energy of the polymer ($E(T_1) = \sim 1.4 \pm 0.05$ eV from triplet sensitization),[44] making this process exoenergetic. This is shown in the Jablonski diagram of Figure 1a that includes the singlet excited-state energies of PF10TBT (1.82 eV), PCBM (1.72 eV), and $PF10TBT^+$:$PCBM^-$ for the 80:20 blend (1.53 eV), and the triplet energy of PCBM (1.50 eV).[49] Charge recombination of the electron on PCBM and the hole on a conjugated polymer into the neutral polymer triplet exciton was previously proposed by Scharber et al.[50] to explain their data for low concentrations of PCBM in MDMO-PPV. Such a process is commonly observed for polymer:polymer blends,[40c,51] and was more recently also described for polythiophene:PCBM blends.[52]

Upon a further increase of the PCBM concentration to 20 and 80 wt %, the triplet absorption intensity reduces, and that of PF10TBT radical cations strongly increases (Figure 8c). At very high PCBM concentration (80 wt %), PF10TBT radical cations completely dominate the PIA spectrum, and PF10TBT triplet excitons no longer contribute significantly.[47] These results are explained with the energy drop of free and weakly bound charge carriers at higher PCBM concentration. The low energy tail of the density of CT states, stabilized by the higher ε_r, shifts to energies below the energy of the neutral PF10TBT triplet exciton ($E(T_1) = 1.4 \pm 0.05$ eV), preventing charge recombination to that neutral PF10TBT triplet excited state, because the CT excitons will instead diffuse to these CT states with lowest energy. We have schematically drawn the density of states (DOS) for CT states in Figure 1b for 20 and 80 wt % PCBM. The maxima in the DOS correspond to the maxima of the CT emission at these concentrations. The broad CT emission implies a distribution of CT states and for the higher PCBM concentrations the low energy tail of the DOS drops below the PF10TBT triplet energy.

In summary the PIA data recorded at 290 K show that at low (10 wt %) PCBM concentration the CT state may decay to the neutral PF10TBT triplet excited state, whereas at higher PCBM concentration the amount of triplet excitons is drastically reduced. The lifetime of the PF10TBT radical cation is significantly enhanced at higher PCBM concentration to 25−30 μs at 80 wt %. The long lifetime indicates minor overlap between the electron and hole wave functions, which we interpret as being due to (trapping at) a large distance. Overall, the PIA data support the proposition made in the previous section that at high PCBM concentration emissive CT states are quenched by forming long-lived charge carriers that eventually recombine nonradiatively.

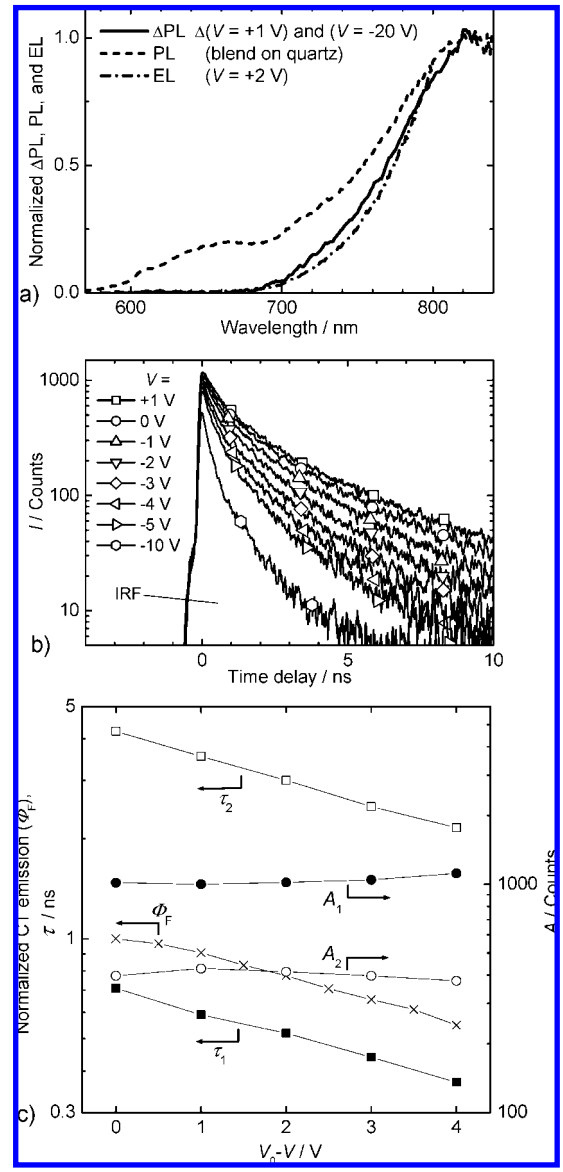

Figure 9. Effect of an applied external electric field on the luminescence of a device containing a thin film of PF10TBT:PCBM with 20 wt % PCBM. (a) Differential PL spectrum at −20 V vs that at +1 V applied bias voltage upon excitation at $\lambda_{exc} = 560$ nm (solid line); the emission is quenched at reverse bias. For comparison the EL spectrum of the same device at +2 V applied bias voltage (dash-dotted line), and the steady state PL spectrum of a thin film on quartz (dashed line) are shown. (b) Field-dependent TR-PL at 780 nm ($\lambda_{exc} = 400$ nm); each trace was collected during 20 min. (c) Results of fits of the TR-PL data in panel b: τ_i (■ and □, left axis) and A_i (● and ○, right axis). Also shown is the steady state CT emission yield at 780 nm normalized to 1 for $V_0 - V = 0$ (×).

G. Quenching of the Singlet CT Exciton by an Electric Field. The PL of a PF10TBT:PCBM 80:20 blend, photoexcited at 560 nm, is quenched upon the application of an externally applied electric field (Figure 9). The differential emission (ΔPL, solid line) measuring at −20 V and +1 V (V_{OC}) in Figure 9a

(49) (a) Williams, R. M.; Zwier, J. M.; Verhoeven, J. W. *J. Am. Chem. Soc.* **1995**, *117*, 4093–4099. (b) Guldi, D. M.; Asmus, K.-D. *J. Phys. Chem. A* **1997**, *101*, 1472–1481.

(50) Scharber, M. C.; Schultz, N. A.; Sariciftci, N. S.; Brabec, C. J. *Phys. Rev. B* **2003**, *67*, 085202.

(51) (a) Ford, T. A.; Avilov, I.; Beljonne, D.; Greenham, N. C. *Phys. Rev. B* **2005**, *71*, 125212. (b) Offermans, T.; Van Hal, P. A.; Meskers, S. C. J.; Koetse, M. M.; Janssen, R. A. J. *Phys. Rev. B* **2005**, *72*, 045213.

(52) Ohkita, H.; Cook, S.; Astuti, Y.; Duffy, W.; Heeney, M.; Tierney, S.; McCulloch, I.; Bradley, D. D. C.; Durrant, J. R. *Chem. Commun.* **2006**, 3939–3941.

shows that the electric field exclusively and quantitatively quenches the CT emission, and not that of the remaining neutral singlet excited states because the ΔPL spectrum has a band shape that is virtually identical to the CT emission spectrum. For comparison a PL spectrum (dashed line) of a 80:20 blend, showing both CT emission and residual PF10TBT and PCBM emission between 600 and 750 nm, is plotted in the same graph. Importantly, the shape of the ΔPL spectrum accurately corresponds to the EL spectrum. At the maximum of the CT emission (820 nm) the quenching amounts to 87% at −20 V relative to +1 V. The PL maximum of the remaining emission has shifted from 820 nm at +1 V to 720 nm at −20 V and hence resembles pure PCBM emission. This shows that at −20 V the CT emission is fully quenched.

We have conducted electric field-dependent TR-PL measurements to investigate whether the quenching of CT emission is a result of a deactivation of excited CT states or if their formation is prevented. Figure 9b shows the corresponding decay traces between 0 and −10 V ($\lambda_{exc} = 400$ nm, $\lambda_{em} = 780$ nm), and reveals that the application of a reverse bias voltage reduces the decay time of the CT emission. Already at a small internal bias (e.g., at $V = 0$ V) the decay is faster than at $V = 1.0$ V (the internal bias in the cell is $V_0 - V$, where $V_0 \approx 1$ V is the compensation voltage at which the net photocurrent is zero, $J_{ph} = J_{light} - J_{dark} = 0$).

Analysis of the TR-PL traces using a biexponential decay reveals that the sum of the pre-exponential factors ($A_1 + A_2$) remains constant, whereas the decay times (τ_1 and τ_2) are gradually reduced with stronger internal electric field (Figure 9c). As a result, the reduction in PL decay time (squares) follows the steady state PL yield (× in Figure 9c). This demonstrates that the field-dependent PL quenching at 780 nm is caused by the dissociation of emissive CT excitons, because an equal amount of CT excitons is created at each applied voltage ($A_1 + A_2$ being constant), and only their decay times (characterized by τ_1 and τ_2) are reduced.

H. Modeling the Field-Dependent and PCBM Concentration-Dependent CT Exciton Dissociation. A model that is frequently used to describe the field-dependent dissociation of CT excitons has been introduced by Braun et al.[7] and is based on Onsager theory. This model can describe the PL quenching of films of conjugated polymers upon application of an electric field,[53] and was recently applied successfully to describe the device characteristics of organic photovoltaic devices.[8,9] In these studies the decay rate of the initially formed CT state to the ground-state was used as a fitting parameter, providing $k_F^{-1} = 2.5-40$ μs.

In the previous sections we demonstrated that the decay time of the initially created emissive CT excitons is typically a few nanoseconds and is reduced in an externally applied electric field (Figure 9). If such a short decay time is used in combination with typical values for the other parameters (R_{CC}, $<\varepsilon_r>$, and $<\mu>$, the spatially averaged sum of electron and hole mobilities) used in the device modeling,[8,9] charge recombination would prevail over dissociation at each applied electric field. This is in strong contrast with the efficient photovoltaic devices prepared from PF10TBT:PCBM blends exhibiting internal quantum efficiencies (IQE) of 75% at short-circuit.[28] We have determined the decay time of the CT exciton experimentally. Hence, we can use this rate at low PCBM concentration ($<\tau> = k_F^{-1} = 4$ ns, Table 2) as a starting point to describe their PCBM concentration- and field-dependent dissociation of CT states.

The probability (P) that a CT state is dissociated can be described by a field dependent dissociation rate k_D and a (field independent) decay rate k_F of the CT state:

$$P(E) = \frac{k_D(E)}{k_D(E) + k_F} \tag{3}$$

Braun derives $k_D(E)$ to be:[7]

$$k_D(E) = k_R \frac{3}{4\pi R_{CC}^3} e^{-E_B/k_B T} \frac{J_1(2\sqrt{-2b})}{\sqrt{-2b}} \tag{4}$$

where R_{CC} is the initial anion-cation separation distance of the charge transfer exciton, $E_B = e^2/4\pi\varepsilon_0\varepsilon_r R_{CC}$ is the binding energy of the CT exciton, k_B is the Boltzmann constant, J_1 is the Bessel function of order 1, and $b = e^3E/8\pi\varepsilon_0\varepsilon_r k_B^2 T^2$. Braun uses Langevin's model for electron−hole recombination which gives $k_R = e<\mu>/\varepsilon_0<\varepsilon_r>$. Following a slight modification of the model of Mihailetchi et al.,[8] we assume a Gaussian distribution of anion−cation separation distances ($x > 0$) around the value of R_{CC} with a width σ to account for disorder in the blends: $F(x) = 1/N \exp(-(x - R_{CC})^2/2\sigma^2)$, with N a normalization factor. Thus eq 3 should be integrated over that distribution:

$$P(E) = \int_0^\infty P(E, x)\, F(x)\, dx \tag{5}$$

This model can be used to fit the field-dependent (Figure 10a), and PCBM concentration-dependent (Figure 10b) quenching of the emissive CT exciton.

We normalize the CT emission intensity to unity for PF10TBT:PCBM blends with 5 and 10 wt % PCBM (Figure 10b). Since at 20 wt % PCBM, the CT emission is 20% lower, we may assume that in this blend 20% of the CT excitons are dissociated at $V_0 - V = 0$ V. In an electric field the CT emission is fully quenched at $V_0 - V = 19$ V (see Section G) and hence we can plot the field-dependent quenching of CT emission as depicted in Figure 10a (closed diamonds). The (dashed, dotted, and dashed-dotted) lines through the data are fits of eq 5 using $k_F^{-1} = 4$ ns (Table 2), and $<\varepsilon_r> = 3.5$[38] as fixed parameters, and $<\mu>$, R_{CC}, and σ as fitting parameters. We find that if values of $<\mu>$ in the range of $0.6-3 \times 10^{-2}$ cm^2 V^{-1} s^{-1} are used with R_{CC} between 1.5 and 2.0 nm, and $\sigma = 0.55$ nm, the CT emission quenching can be accounted for. A value of R_{CC} on the order of 1.5 nm is an anticipated electron−hole separation distance in a CT exciton. The relatively high value of $<\mu>$ can be interpreted as being mainly determined by the high electron mobility in PCBM clusters. The electron mobility in a microcrystalline PCBM powder is $\mu_e = 8.0 \times 10^{-2}$ cm^2 V^{-1} s^{-1} (by flash-photolysis time-resolved microwave conductivity, FP-TRMC),[54] which is much higher than the hole mobility of PFTBT ($\mu_h = 6-8 \times 10^{-5}$ cm^2 V^{-1} s^{-1} from SCLC measurements available only).[25,26] The value of μ_e determined by FP-TRMC is 3−40 × higher than those obtained by SCLC measurements,[34,55–57] which is generally explained by the fact that the TRMC measurements probe the *local* electron mobility inside a PCBM crystal, whereas by SCLC the mobility through

(53) (a) Goliber, T. E.; Perlstein, J. H. *J. Chem. Phys.* **1984**, *80*, 4162–4167. (b) Jung, J.; Glowacki, I.; Ulanski, J. *J. Chem. Phys.* **1999**, *110*, 7000–7007. (c) Pan, J.; Scherf, U.; Schreiber, A.; Haarer, D. *J. Chem. Phys.* **2000**, *112*, 4305–4309.

(54) Savenije, T. J.; Kroeze, J. E.; Wienk, M. M.; Kroon, J. M.; Warman, J. M. *Phys. Rev. B* **2004**, *69*, 155205.

(55) Tuladhar, S. M.; Poplavskyy, D.; Choulis, S. A.; Durrant, J. R.; Bradley, D. D. C.; Nelson, J. *Adv. Funct. Mater.* **2005**, *15*, 1171–1182.

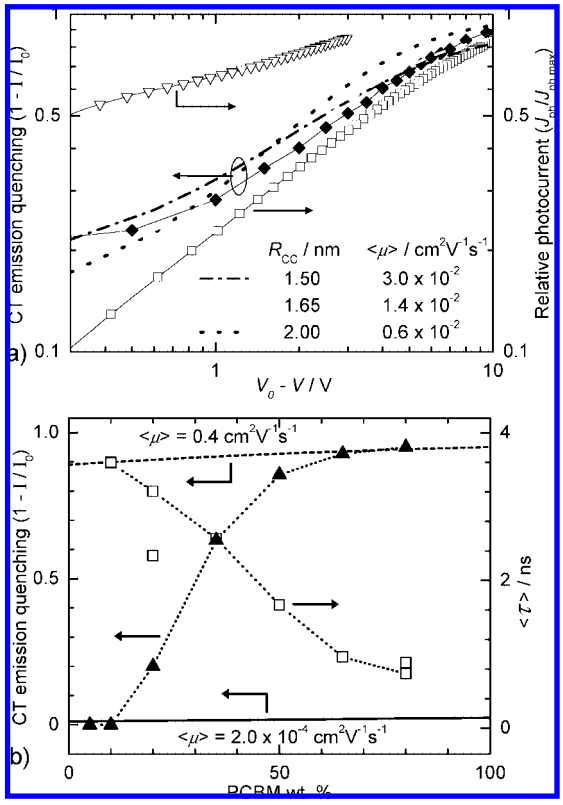

Figure 10. (a) Fits (lines, left axis) of eq 5 to the field-dependent PL quenching of the CT emission (♦, left axis) of the device containing 20 wt % PCBM assuming 20% quenching at $V_0 - V = 0$ and 100% quenching at −20 V. Parameters used for the fit were $k_F^{-1} = 4$ ns, $<\varepsilon_r> = 3.5$, $\sigma = 0.55$ nm, and $<\mu>$ and R_{CC} are indicated in the graph. $J_{ph}-V$ curves (right axis) of devices containing PF10TBT:PCBM blends with 20 (□) and 80 (▽) wt % PCBM are also plotted. The photocurrent was corrected for the dark current ($J_{ph} = J_{light} - J_{dark}$) prior to the analysis. (b) Normalized PL quenching at the peak wavelength (▲, left axis) and average decay time at 780 nm (□, right axis, Table 2) of the CT emission in PF10TBT:PCBM blends as a function of the PCBM concentration. The PL data of one series is connected by dotted lines. The dashed line indicates the zero-field quenching of CT emission for high PCBM concentration as predicted by eq 5 using $E = 0$, $<\mu> = 0.4$ cm^2 V^{-1} s^{-1}, $R_{CC} = 2.5$ nm, and $\sigma = 0.55$ nm. The solid line is a prediction that uses the same values except for $<\mu>$ which was set to 2.0×10^{-4} cm^2 V^{-1} s^{-1}. For both predictions $<\varepsilon_r>$ is varied between 3.4 and 4.0 for 0−100 wt % PCBM.

a complete layer (including grain boundaries) is probed. It can be argued that for describing the field dependent dissociation of CT states, the local mobility is a more descriptive parameter than the device mobility.

The size of PCBM clusters, which is not included in the model, is expected to have a major effect on CT state dissociation. The capture radius ($r_c = k_B 4\pi\varepsilon_0\varepsilon_r T/e^2$), being the distance that an electron should travel before it can escape the attraction from the hole, amounts to $r_c = 15 \pm 1$ nm for the relative permittivity ($\varepsilon_r = 3-4$) in these blends at room temperature, and gives a minimal length scale over which the high electron mobility should be attained to ensure efficient CT dissociation.

The model is able to follow the observed quenching of CT emission down to $V_0 - V \approx 0$ at which about 20% of the CT states are dissociated. The PL quenching curve can be compared to the photocurrent density measured on the same device, normalized to unity at high reverse bias (Figure 10a, squares). We find that the normalized photocurrent is always lower than the quenching ($1 - I/I_0$) of the emissive CT exciton. Thus, although we stress that the absolute initial quantum yield of the (emissive) CT excitons is not known, it is possible that these states are precursors to all charge carriers extracted from the device. Following this interpretation the offset between the yield of extracted charge carriers and the quenching of CT emission can be explained by recombination losses. At low electric fields ($V_0 - V$) the charge carriers move mainly via diffusion in either direction and thus have a long residence time, giving ample time for bimolecular decay (e.g., to neutral triplet states or the ground state) or collection at the "wrong" electrode, and explaining the relatively large offset between the quenching of CT emission and photocurrent.

Having analyzed the field-dependent quenching of the CT emission, we now consider the PCBM concentration-dependent quenching of the CT exciton (Figure 4d) in absence of an electric field. After normalization of the PL yield of the CT emission for the blends containing 5 and 10 wt % PCBM, eq 5 -in absence of an electric field $J_1(2\sqrt{-2b})/\sqrt{-2b} = 1$- can be used to analyze the data (Figure 10b), assuming that dissociated CT excitons have a much lower probability to recombine radiatively. The high amount of CT emission quenching at 65 and 80 wt.% PCBM can be explained when large values of R_{CC} and $<\mu>$ are used. For example the dashed line in Figure 10b is obtained by using $R_{CC} = 2.5$ nm, $\sigma = 0.55$ nm and $<\mu> = 0.4$ cm^{2}V^{-1}s^{-1}. It is interesting to compare this result with those of recent optical methods determining charge carrier mobilities in films containing PCBM in the subpicosecond time domain. High charge (electron and/or hole) mobility in PCBM films were found on the order of 0.1 cm^2 V^{-1} s^{-1},[58] and a mechanism of fast carrier drift toward interdomain boundaries is proposed.[58,59] This allows the electron on PCBM to escape from geminate recombination if it is in such a cluster. Oppositely, to explain the lack of quenching of CT emission at low PCBM concentration, a low value of $<\mu>$ in the order of 10^{-4} cm^2 V^{-1} s^{-1} must be used. The strong increase of $<\mu>$ with PCBM concentration is consistent with the expectation that the electron mobility in PCBM clusters is higher than the hole mobility in the PF10TBT phase.

Since the high μ_e of PCBM is related to the presence of microcrystalline clusters, these play a crucial role in effectively separating the charge carriers by ensuring a high $<\mu>$. Hence,

(56) For PCBM macroscopic electron mobilities (μ_e) have been reported of $0.45-20 \times 10^{-2}$ (field effect mobilities, ref 57a−d) and $0.2-3.3 \times 10^{-2}$ cm^2 V^{-1} s^{-1} (space-charge-limited current, SCLC refs 34 and 55). Local electron mobilities inside PCBM nanocrystals have been reported of $\mu_e = 8 \times 10^{-2}$ cm^2 V^{-1} s^{-1} (by flash-photolysis time-resolved microwave conductivity, FP-TRMC, ref 54) and for the sum of the electron and hole mobility: $\Sigma\mu_{min} = 4-30 \times 10^{-2}$ cm^2 V^{-1} s^{-1} (pulse-radiolysis TRMC, ref 35).

(57) (a) Anthopoulos, T. D.; Tanase, C.; Setayesh, S.; Meijer, E. J.; Hummelen, J. C.; Blom, P. W. M.; De Leeuw, D. M. *Adv. Mater.* **2004**, *16*, 2174–2179. (b) Waldauf, C.; Schilinsky, P.; Perisutti, M.; Hauch, J.; Brabec, C. J. *Adv. Mater.* **2003**, *15*, 2084–2088. (c) Meijer, E. J.; De Leeuw, D. M.; Setayesh, S.; Van Veenendaal, E.; Huisman, B.-H.; Blom, P. W. M.; Hummelen, J. C.; Scherf, U.; Kadam, J.; Klapwijk, T. M. *Nat. Mater.* **2003**, *2*, 678–682. (d) Singh, T. B.; Marjanovic, N.; Stadler, P.; Auinger, M.; Matt, G. J.; Günes, S.; Sariciftci, N. S.; Schwödiauer, R.; Bauer, S. *J. Appl. Phys.* **2005**, *97*, 083714.

(58) Cabanillas-Gonzalez, J.; Virgili, T.; Gambetta, A.; Lanzani, G.; Anthopoulos, T. D.; De Leeuw, D. M. *Phys. Rev. Lett.* **2006**, *96*, 106601.

(59) Barbour, L. W.; Hegadorn, M.; Asbury, J. B. *J. Am. Chem. Soc.* **2007**, *129*, 15884–15894.

the increased performance at high PCBM concentration is directly associated with the presence of larger PCBM crystals in the blends and the possibility of electrons to escape beyond the capture radius.

The quenching of CT exciton emission in a blend containing 80 wt % of PCBM, without any applied electrodes ($1 - I/I_0 = 0.9$, Figure 10b), can be explained by CT exciton dissociation using the Braun model, and is high enough to explain the photocurrent ($J_{ph}/J_{ph,max} = 0.5$, Figure 10a) of the device with the same fullerene content at low applied electric field ($V_0 - V = 0.1$ V).[60] Hence, this enhanced CT exciton dissociation allows for high photocurrents when the cell is operated close to V_{OC}. This is a prerequisite to achieve a high fill factor.

IV. Conclusions

The performance of photovoltaic devices made from blends of PF10TBT and PCBM strongly depends on the PCBM concentration, which we have related to the formation of larger PCBM clusters at high fullerene content. In the ground-state absorption spectra of these blends we observe an additional band which is attributed to a ground-state CT transition. The formation and decay of emissive CT excited states via electron transfer from photoexcited PF10TBT or PCBM (Figure 1a) in these blends is confirmed by steady state and time-resolved photoluminescence measurements. The CT states can also be created electrically in electroluminescent devices prepared from PF10TBT:PCBM blends.

At low PCBM concentration, the CT emission has an average decay time of about $<\tau> = 4$ ns. The emission intensity and lifetime of these CT states are strongly reduced by the application of an external electric field for a blend containing 20 wt % PCBM, and is also effectively quenched at higher PCBM concentrations in blends without any applied electrodes. Additionally, the CT emission shifts to lower energy with increasing PCBM concentration. The reduction of the energy (E_{CT}) of the CT states for increasing PCBM concentration correlates with the open-circuit voltage of photovoltaic devices prepared from these blends by $V_{OC} = (1/e)(E_{CT} - 0.45 \pm 0.05$ eV), if E_{CT} is determined from the maximum CT emission. The higher relative permittivity (ε_r) of PCBM compared to that of PF10TBT quantitatively explains the reduction of E_{CT}, as inferred from a continuum model (eq 1), and also infers a lower energy for free charge carriers, influencing the V_{OC} (eq 2). Finally, we find that at low PCBM concentration CT states recombine to the triplet state of PF10TBT. At high PCBM concentrations, however, the tail of the energetic distribution of CT states drops below that of the PF10TBT triplet, which inhibits this additional recombination pathway of CT states. The higher ε_r of PCBM, which reduces E_{CT}, thereby enables formation of longer-lived charge carriers, possibly having a favorable effect on the device efficiency, because they can more easily be extracted.

The concentration- and field-dependent quenching of CT emission can be accounted for by an Onsager−Braun model assuming high average charge carrier mobility in the vicinity of the dissociating CT exciton. This high mobility can be interpreted in terms of an electron mobility in PCBM clusters in the order of $\mu_e = 0.1$ cm^2 V^{-1} s^{-1}. We find that the sum of the field-independent and field-dependent quenching of CT emission is always larger than the amount of photocurrent relative to the maximum photocurrent at high reverse bias. This allows for the possibility that each extracted charge carrier has passed through the CT state with an intrinsic lifetime of $<\tau> = 4$ ns. Notably, for a blend with 80 wt % PCBM ca. 90% of the emissive CT states is dissociated into free charge carriers without any applied electrodes.

The experimental recombination time of the CT exciton of $<\tau> = k_F^{-1} = 4$ ns in the PF10TBT:PCBM blend is 3 orders of magnitude less than typical values found in polymer:PCBM blends by fitting the $J-V$ curves when using charge carrier mobilities that represent the macroscopic transport through the blends.[8−11] The Onsager−Braun model can reconcile such a short lifetime of the interfacial CT state with the high IQE = 75%,[25,28] only when a relatively high local charge carrier mobility (on the order of 0.1 cm^2 V^{-1} s^{-1}) exists. Because the absolute initial quantum yield of the (emissive) CT excitons is not known, a contribution of directly formed free charge carriers cannot be excluded.

We further note that also in other polymer:PCBM blends, where CT emission is not observed because of low intensity, or because it may appear in a region where detection is usually less sensitive (>850 nm), CT excitons may exist. Actually, CT *absorption* is commonly observed for polymer:PCBM blends.[20,33] Hence, also here the dissociation of CT excitons into more free charge carriers by high mobility, crystalline polymer or PCBM phases is a possible mechanism.

From this work we further conclude that the improved device efficiency of the PF10TBT:PCBM devices with larger phase separation is closely related to an improved separation of bound electron−hole pairs at the donor−acceptor interface due to formation of PCBM crystals. While the improvement of charge transport by domain formation and crystallization of either donor or acceptor has often been used to explain the improved device performance,[3,4,61−63] we note that this study reveals that domain formation enhances the generation of free charge carriers.[6a−d] This conclusion is supported by the result that also for conjugated polymer:polymer blends, a reduction of CT emission and enhanced performance is observed when increased phase separation is induced by thermal annealing.[63] Apparently, a lowering of the interface area upon phase separation is effectively counteracted by more facile generation of free charge carriers.

Altogether the presented data support the hypothesis that the presence of PCBM clusters is crucial for efficient generation of free charge carriers in photovoltaic devices prepared from blends of conjugated polymers and PCBM, as the high local

(60) The IQE estimated from $J_{ph}/J_{ph,max} = \sim 25\%$ of the 20 wt % blend at short circuit ($V_0 - V \approx 1$ V) is in agreement with the lower device efficiency device compared to $J_{ph}/J_{ph,max} = 65\%$ for the 80 wt % PCBM device. $J_{ph}/J_{ph,max} = 65\%$ agrees with an IQE = 55−75% for this polymer blend (ref 28).

(61) Xue, J.; Rand, B. P.; Uchida, S.; Forrest, S. R. *Adv. Mater.* **2005**, *17*, 66–71.
(62) (a) Dittmer, J. J.; Marseglia, E. A.; Friend, R. H. *Adv. Mater.* **2000**, *12*, 1270–1274. (b) Nakamura, J.; Yokoe, C.; Murataa, K.; Takahashi, K. *J. Appl. Phys.* **2004**, *96*, 6878–6883.
(63) (a) Veenstra, S. C.; Verhees, W. J. H.; Kroon, J. M.; Koetse, M. M.; Sweelssen, J.; Bastiaansen, J. J. A. M.; Schoo, H. F. M.; Yang, X.; Alexeev, A.; Loos, J.; Schubert, U. S.; Wienk, M. M. *Chem. Mater.* **2004**, *16*, 2503–2508. (b) Kietzke, T.; Hörhold, H.-H.; Neher, D. *Chem. Mater.* **2005**, *17*, 6532–6537. (c) Koetse, M. M.; Sweelssen, J.; Hoekerd, K. T.; Schoo, H. F. M.; Veenstra, S. C.; Kroon, J. M.; Yang, X.; Loos, J. *Appl. Phys. Lett.* **2006**, *88*, 083504.

electron mobility in these clusters enables the efficient dissociation of short-lived CT excitons that may otherwise recombine radiatively or nonradiatively.

Acknowledgment. We would like to thank Dr. M. Kemerink for stimulating discussions on device-related issues, and Dr. J. W. Stouwdam for support with the EL measurements. This work was supported by the EU Integrated Project NAIMO (No. NMP4-CT-2004-500355).

Supporting Information Available: Absorption, steady-state and time-resolved photoluminescence, and PIA spectra of PF10TBT:PCBM films. This material is available free of charge via the Internet at http://pubs.acs.org.

JA8012598